

Social Returns to Conservation: Incentives for Cover Crops and Water Quality in the Midwest^{*}

Shuo Yu[†]

This version: October 22, 2025

[Click here for the latest version](#)

Abstract

This study estimates the effectiveness of the U.S. Department of Agriculture's Environmental Quality Incentives Program (EQIP) cover crop subsidy program to mitigate water pollution from agricultural runoff and leaching. The study uses a novel satellite-derived dataset of field-level cover crop adoption and exploits quasi-experimental variation from the geographically and temporally varying implementation of EQIP's Mississippi River Basin Healthy Watersheds Initiative (EQIP-MRBI). Event-study results show that MRBI funding raises cover crop adoption by 29% above baseline, with persistent effects. Linking the satellite adoption data to water-quality records, the study finds that a one-percentage-point increase in upstream adoption reduces total nitrogen by 0.83%. The implied benefit–cost ratio is 2.52.

Keywords: EQIP, Water Quality, Cover Crops, Satellite Data, Agricultural Policy

JEL Codes: Q58, Q53, Q15, C33

*I am deeply grateful to Jeffrey M. Perloff for his guidance and support throughout this project. I am especially thankful to Aprajit Mahajan, Joseph S. Shapiro, Aaron Smith, and Brian Wright for their generous advice and encouragement. Special thanks go to Timothy M. Bowles for sharing data and valuable insights. I also thank Francis Annan, Ellen Bruno, Leila Njee Bugha, Chi Man Cheung, Abdoulaye Cissé, Alexandra Hill, Jie Song, Elif Tasar, Sofia Berto Villas-Boas, Arthur R. Wardle, and David Zilberman for their helpful comments and discussions. Special thanks to the attendees of the UC Berkeley Leo Simon ANR Seminar, the UC Berkeley Sara Johns EERE Workshop, the Columbia University Interdisciplinary Workshop in Sustainable Development, the University of San Francisco Economics Seminar, Camp Resources, AAEA, WEAI, AERE, and CES North American conferences for their helpful discussions. Financial support from a Giannini Foundation mini-grant is gratefully acknowledged. All remaining errors are my own. In loving memory of Sara Johns.

[†]S. Yu: Department of Agricultural and Resource Economics, UC Berkeley. Email: shuoy@berkeley.edu.

1 Introduction

Agricultural runoff and leaching are major sources of nonpoint source water pollution in the Midwest. To mitigate this problem, the U.S. Department of Agriculture (USDA) Environmental Quality Incentives Program (EQIP) subsidizes non-cash cover crops during the off-season. Cover crops have the potential to improve soil health and reduce runoff and leaching. This study estimates the social returns to EQIP by examining the program's effectiveness in incentivizing cover crop adoption, thereby improving water quality. It assesses the cost-effectiveness of EQIP subsidies by comparing program expenditures to the social benefits from reduced nutrient pollution.

Agriculture's fertilizer losses through surface runoff and subsurface leaching play a central role in nonpoint source water pollution in the Midwest. The resulting nutrient pollution, primarily from excessive nitrogen and phosphorus, causes harmful algal blooms and hypoxic "dead zones," and poses public health risks (e.g., [Dodds et al., 2009](#); [Kudela et al., 2015](#); [Ward et al., 2018](#)).

In theory, a Pigouvian tax on nutrient runoff would be the first-best instrument to internalize pollution externalities. In practice, however, the diffuse nature of agricultural emissions makes it nearly impossible to monitor and attribute nutrient loads to individual farms. Consequently, nonpoint source pollution from runoff and leaching is largely exempt from regulation under the Clean Water Act. Mitigation, therefore, relies primarily on incentive-based approaches, such as conservation subsidies, to encourage environmentally beneficial conservation practices.

Instead, the U.S. government subsidizes cover cropping, which improves soil health and reduces nutrient losses to waterways, among a range of additional agronomic and environmental benefits (e.g., [Sharpley and Smith, 1991](#); [Blanco-Canqui, 2018](#); [Chen et al., 2022](#)). Despite these benefits, few farmers adopt cover crops without subsidies. Cover crops entail annual variable costs for seeds, labor, and management, as well as additional learning and adjustment costs during the initial adoption period. Meanwhile, the private benefits for farmers, such as soil health, higher subsequent cash crop yields, and reduced production risks, typically show up after three to five years of adoption. As a result, financial incentives are often necessary to help farmers overcome the upfront learning costs and information frictions associated with adoption.

EQIP is the largest working-lands conservation incentive program in the United States¹

¹In U.S. conservation policy, working-lands programs are initiatives that allow landowners to continue agricultural production while adopting conservation practices (e.g., cover cropping and reduced tillage). By contrast, land-retirement programs like the Conservation Reserve Program (CRP) pay landowners to remove cropland from production for a fixed contract period and convert it to conservation uses. These two

and one of the largest Payments for Ecosystem Services (PES) mechanisms worldwide². EQIP's annual financial assistance has expanded from about \$0.8 billion in 2014 to over \$2.6 billion in 2024, supporting farmers who voluntarily adopt conservation practices to improve soil, water, and ecosystem health. Among these practices, cover cropping is the largest payment category, with more than \$1.4 billion allocated since 2014.

Despite the growing scale of EQIP, empirical evidence on whether such subsidies translate into meaningful reductions in nutrient pollution across states or regions remains limited. Moreover, concerns remain that environmental priorities may not be the primary driver of EQIP funding allocations across and within states, raising questions about the program's cost-effectiveness ([USDA OIG, 2014](#); [GAO, 2017](#)). These questions have become even more salient in light of recent policy developments. The 2022 Inflation Reduction Act (IRA) allocated \$8.45 billion in new EQIP funding for FY 2023–2026, more than doubling the program's budget. However, the Trump administration has since frozen the disbursement of these IRA conservation funds beginning in 2025, fueling renewed debate over whether taxpayer dollars should continue to support EQIP conservation efforts.

We focus on the EQIP's Mississippi River Basin Healthy Watersheds Initiative (EQIP–MRBI), a major sub-initiative covering 12 states along the Mississippi River. It provides additional EQIP funding to targeted subwatersheds within pre-designated priority subbasins³. Through MRBI, the USDA Natural Resources Conservation Service (NRCS) targets high-nutrient areas to improve water quality outcomes. The initiative's dynamic treatment assignment, with funding that can turn on and off across subwatersheds and years, provides a quasi-experiment.

Our main contribution is to causally quantify the environmental effectiveness and cost-effectiveness of federal conservation incentives in the Midwest. To conduct this analysis, we construct an innovative dataset that integrates field-level cover crop adoption data from satellite imagery and machine learning models, EQIP–MRBI policy boundaries and payments, and surface water-quality measurements, along with auxiliary environmental variables on hy-

types of programs, therefore, face distinct economic trade-offs: the working-land programs involve recurring variable and maintenance costs each year, whereas land-retirement programs tend to impose a more fixed-cost structure, i.e., mainly the opportunity cost of foregone production and, sometimes, restoration costs when the contract ends. See [Aillery \(2006\)](#) and [Feng et al. \(2006\)](#) for comparative frameworks analyzing working-land versus land-retirement programs.

²PES are arrangements in which land managers receive compensation for practices that provide or maintain ecosystem services such as clean water, carbon storage, or biodiversity. The EQIP is a government-financed PES program. See [Kinzig et al. \(2011\)](#) and [Salzman et al. \(2018\)](#) for comprehensive discussions of PES programs.

³The U.S. Geological Survey (USGS) divide the nation's landscape into nested hydrologic units that represent drainage areas of varying scales. Each hydrologic unit is identified by a unique Hydrologic Unit Code (HUC). Among these, HUC-8 subbasins denote medium-scale river basin areas, while HUC-12 subwatersheds represent smaller catchments nested within subbasins. See Appendix B.3 and Figure 2 for details.

dology, weather, and soil characteristics. Exploiting the quasi-experimental variation from the staggered activation of EQIP–MRBI funding across subwatersheds, an event-study design shows that program funding increases cover crop adoption by 29% from the baseline level. In contrast to findings from previous studies, this adoption effect exhibits limited additionality but largely persists after funding ends. We then evaluate the effects of cover crops on water pollution using panel data analysis, where the upstream cover crop adoption share serves as the main explanatory variable and the downstream share functions as a placebo test. The specification includes subwatershed-by-year fixed effects to account for time-varying targeting policies directed at subwatersheds. The results indicate that a one-percentage-point increase in upstream adoption reduces total nitrogen concentrations by 0.83%. Combining both estimates, we calculate a benefit–cost ratio of 2.52. These findings demonstrate that federal conservation subsidies can be highly cost-effective while highlighting the importance of improved program targeting to enhance environmental outcomes.

We compile data from six sources. First, we construct field-level cover crop adoption data using Landsat satellite imagery, USDA surveys, windshield ground-truth datasets, and machine learning algorithms. This approach extends previous methodologies by incorporating a larger and more diverse training dataset, employing advanced vegetation indices, enhancing data preprocessing, and using ensemble models, thereby improving upon [Seifert et al. \(2018\)](#). The resulting dataset achieves an out-of-sample classification accuracy of 95.1%. Assembling new data on cover crop adoption helps overcome a key limitation of existing research on conservation programs, namely the lack of consistent, large-scale measures of adoption. It enables causal analysis linking EQIP–MRBI funding to cover crop adoption at the subwatershed level and, subsequently, linking finer-scale adoption within subwatersheds to water quality outcomes.

Second, we obtain information on EQIP–MRBI policy design, targeting areas over time, and funding intensity at the subbasin level through multiple Freedom of Information Act (FOIA) requests to the USDA NRCS. Third, we use water quality data for the Mississippi–Atchafalaya River Basin from [Krasovich et al. \(2022\)](#), which provide detailed and harmonized daily measurements of nitrogen and phosphorus concentrations across the Midwest. Fourth, we incorporate data on hydrologic units and water flow directions from the National Hydrography Dataset to link field-level cover crop adoption with upstream and downstream catchments of water monitoring stations. Finally, for control variables and heterogeneity analyses, we draw on auxiliary datasets, including gridded climate data from the Parameter-elevation Regressions on Independent Slopes Model (PRISM) as used in [Schlenker and Roberts \(2009\)](#), land use data from the USDA Cropland Data Layer (CDL), and soil characteristics from the USDA gridded National Soil Survey Geographic Database (gNATSGO).

To estimate EQIP’s effect on cover crop adoption over time, the paper exploits the temporal variation in EQIP–MRBI funding, which provides additional EQIP assistance to targeted subwatersheds within priority subbasin. We conduct event studies comparing subwatersheds eligible for MRBI funding (treatment group) with subwatersheds in the same priority subbasins that have not yet entered MRBI implementation (control group). The empirical strategy follows the difference-in-differences framework of [de Chaisemartin and D’Haultfoeuille \(2024\)](#), which allows for settings with dynamic treatment timing, reversible (non-absorbing) treatment status, and lagged treatment effects.

Results from six Midwestern states show that one year of MRBI funding increases cover crop adoption by 1.75 percentage points in total on average from a baseline of 6%, representing a 29% increase. Two key dimensions for evaluating the effectiveness of PES programs are persistence, which refers to the extent to which conservation practices continue after program funding ends, and additionality, which captures the degree to which subsidized practices represent genuine new adoption that would not have occurred otherwise. The effects of MRBI funding on cover crop adoption emerge gradually after the initiative begins and remain positive and statistically significant for up to eleven years after the first treatment year, indicating persistent adoption over time. However, when comparing the estimated additional adoption acreage to the total acreage that the average subwatershed investment under MRBI could support, only about 20% of the subsidized adoption represents additional conservation, suggesting limited program additionality.

After establishing that the subwatershed targeting policy effectively incentivizes additional cover crop adoption, this paper examines how cover crop adoption affects surface water quality. The analysis aggregates the share of fields adopting cover crops upstream and downstream of each monitoring station within the same subwatershed. The outcome variables are measures of surface water quality, specifically the concentrations of nitrogen and phosphorus compounds. Since only cover crops in the upstream catchment can influence water quality at the monitoring station, the upstream adoption share serves as the key explanatory variable. Downstream adoption, which cannot plausibly affect water readings, is used as a placebo test to detect unobserved heterogeneity within subwatersheds, such as localized NGO activities or conservation initiatives. The specification also includes subwatershed-by-year fixed effects to account for time-varying subwatershed targeting policies. The key identification assumption is that the spatial location of fields adopting cover crops is exogenous to the location of the water quality monitoring station, given the total acreage adopting cover crops in a subwatershed. The results show that a one-percentage-point increase in upstream cover crop adoption reduces total nitrogen levels by 0.83%, while the effect on phosphorus concentrations is statistically insignificant.

This research highlights the potential of EQIP to drive conservation while raising important questions about its efficiency and targeting. The cost–benefit analysis indicates that cover crop subsidies reduce nitrogen pollution, with an estimated benefit–cost ratio of 2.52. This sizable return underscores both the environmental value of EQIP and the importance of improving targeting and cost-effectiveness in program design. Given the observed low level of additionality in cover crop adoption, future conservation efforts may benefit from improved targeting strategies. These findings contribute to the broader discussion on designing effective PES programs to maximize environmental impact and economic viability.

Related Literature. This study contributes to four main strands of the literature. First, this paper builds on the literature examining the additionality and persistence of Payment for Ecosystem Services (PES) programs. Our contributions are twofold: (1) we provide the first large-scale, satellite-based empirical evidence on persistence of conservation adoption in an agricultural PES context, and (2) we document new evidence of limited additionality in EQIP. The most directly relevant studies are [Rosenberg et al. \(2025\)](#) and [Larson \(2024\)](#), which analyze EQIP’s impacts on cover crop adoption using administrative and self-reported data. Because cover crop reporting is voluntary, these datasets suffer from substantial missing values and cover only a short panel period, limiting their ability to evaluate persistence precisely. Nevertheless, in contrast to our findings, the authors report substantially higher additionality of EQIP participation. In another context, [Aspelund and Russo \(2023\)](#) employs satellite-based crop choice data and a regression discontinuity design to study additionality in the Conservation Reserve Program, a land-retirement program that allocates contracts through a procurement auction. Additionally, persistence in the CRP context differs conceptually from that in EQIP because the underlying cost structures and incentives are distinct. Other studies using survey data at more local scales also report high additionality, ranging from 54% to 98% (e.g., [Fleming, 2017](#); [Fleming et al., 2018](#); [Claassen et al., 2018](#); [Sawadgo and Plastina, 2021](#)).

Second, this paper contributes to the literature on the cost-effectiveness of PES programs. It develops a cost–benefit analysis framework for EQIP cover crop subsidies that relies on a quasi-experimental causal design at the regional scale. Much of the existing evidence on PES cost-effectiveness comes from developing-country and forest-sector contexts, where randomized controlled trials (RCTs) are more feasible. For example, [Jack \(2013\)](#) and [Jack and Jayachandran \(2019\)](#) examine how contract design, targeting, and self-selection shape the cost-effectiveness of PES interventions. While these studies provide valuable insights, they remain largely outside the U.S. working-lands context. Within the United States, the USDA has traditionally relied on the Conservation Effects Assessment Project (CEAP), which uses

simulation-based integrated assessment models to evaluate program cost-effectiveness (USDA NRCS, 2022). While these models are practical for nationwide policy evaluation, they are difficult to validate empirically and may not accurately reflect real-world adoption behavior. Recent empirical studies, such as Liu et al. (2023), evaluates cost-effectiveness using panel data and aggregated administrative records, though identification challenges remain.

Third, this paper provides new causal evidence on how conservation land management affects nonpoint source (NPS) water pollution at scale. While field-level plot studies such as Lee et al. (2003) have demonstrated how conservation practices affect runoff, econometric analysis of agricultural NPS pollution remains relatively limited as noted in Keiser et al. (2019). Recent empirical studies typically rely on aggregated data at watershed or subbasin scales, which raises concerns about unobserved correlation between program targeting and pollution outcomes (Liu et al., 2023; Metaxoglou and Smith, 2025; Hsieh and Gramig, 2024; Karwowski and Skidmore, 2023; Zhang et al., 2025).

Finally, it contributes to the broader literature on the environmental benefits of cover crops by quantifying their social returns in terms of water-quality improvements and cost-effectiveness. Agronomic studies have long documented their potential to improve soil health, reduce erosion, and limit nutrient loss (Blanco-Canqui, 2018; Dabney et al., 2001; Fageria et al., 2005; Kaye and Quemada, 2017; Sarrantonio and Gallandt, 2003; Tonitto et al., 2006; Chen et al., 2022). More recent work has explored their role in climate mitigation and nutrient management (Won et al., 2024; Aglasan et al., 2024; Ma et al., 2023; Hsieh and Gramig, 2024).

Outline. The rest of the paper is organized as follows. Section 2 provides an overview of the institutional background of the EQIP and MRBI, as well as nutrient pollution and the mitigation role of cover crops. Section 3 describes the data used in the analysis. Section 4 presents findings on the causal effects of EQIP funding on cover crop adoption. Section 5 presents our results on the impact of cover crop adoption on surface water quality. Section 6 discusses the cost-effectiveness of EQIP–MRBI investments. Section 7 provides concluding remarks.

2 Background and Institutional Setting

2.1 EQIP and MRBI

EQIP, administered by the USDA NRCS, provides financial and technical assistance to farmers and landowners to implement conservation practices. Funding for cover crops under

EQIP has expanded markedly since 2009, making it the largest single practice category, with total obligations exceeding \$1.4 billion since 2014.

The program's stated goal is to optimize environmental benefits, though previous evaluations have questioned its cost-effectiveness and targeting of environmental outcomes ([USDA OIG, 2014](#); [GAO, 2017](#)). In practice, to fulfill this goal, the USDA NRCS first allocates EQIP funds from the federal to the state level based on national priorities. Farmers apply through local NRCS offices, and state offices rank applications according to federal, state, and local environmental priorities. Selected applicants sign multi-year contracts to implement approved conservation practices and receive payments, typically after the practices are completed. (Additional details on EQIP mechanisms are provided in Appendix [B.1](#).)

In this paper, we focus on the EQIP–MRBI for two main reasons. First, MRBI is one of the few major EQIP initiatives specifically designed for the Mississippi River Basin. This region is both central to U.S. agriculture and a significant source of nutrient runoff that contributes to Gulf hypoxia (a recurring low-oxygen region that forms each summer where the Mississippi and Atchafalaya Rivers discharge into the Gulf of Mexico).

Second, the initiative's design provides a quasi-experimental setting for rigorous evaluation. Building on the EQIP framework, the MRBI provides additional financial and technical assistance to support conservation practices (e.g., cover cropping) in targeted subwatersheds to reduce agricultural runoff and improve water quality. For each cohort, USDA NRCS designates priority zones at the Hydrologic Unit Code 8 (HUC-8) or subbasin level⁴. State NRCS offices review partner proposals and select projects for MRBI funding, targeting HUC-12 subwatersheds within priority zones that exhibit high pollution levels and strong potential to affect downstream nutrient runoff (see Appendix [B.2](#)). This targeting creates a quasi-experiment setting: subwatersheds selected for projects serve as treatment units, while non-selected subwatersheds within the same priority zones provide credible controls.

Figure 1 summarizes the spatial and temporal variations of MRBI implementation. Panel [1a](#) maps the MRBI 2025 priority areas across the Mississippi River Basin, where the green polygons represent subwatersheds selected for implementation and the yellow polygons indicate subbasin-level priority zones designated by the USDA NRCS. Panel [1b](#) documents the number of subwatersheds entering implementation each year.

2.2 Cover Crops and Water Quality

Nitrogen and phosphorus, key nutrients for crop growth, are major components of commercial fertilizers but contribute to serious environmental and economic problems when overapplied.

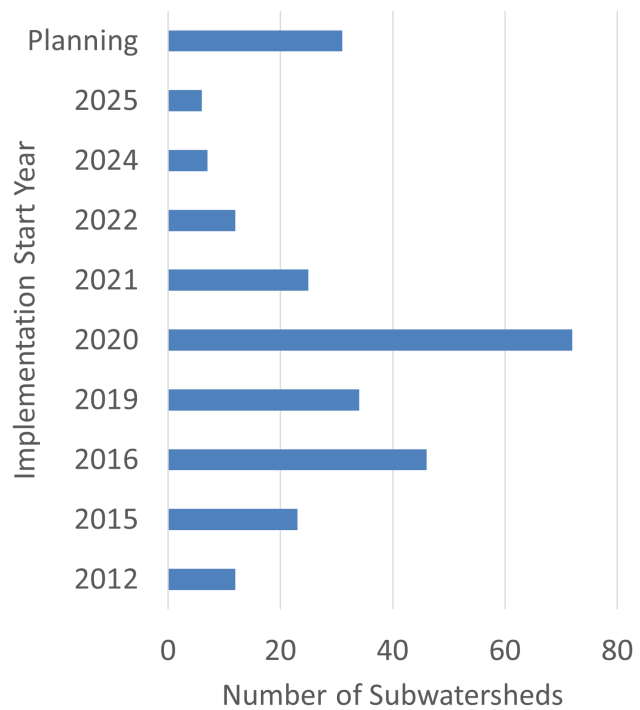
⁴Hydrologic units are standardized watershed boundaries defined by the U.S. Geological Survey. HUC-12 subwatersheds nested within HUC-8 subbasins. See Appendix [B.3](#) and Figure [2](#) for details.

Figure 1: EQIP–MRBI Geographic Scope and Distribution of Implemented Subwatersheds

(a) 2025 EQIP–MRBI Implemented Subwatersheds



(b) Implementation Timeline of Subwatersheds



Note: This figure shows the geographic extent of the 2025 Mississippi River Basin Healthy Watersheds Initiative (MRBI) priority areas (panel a) and the distribution of priority subwatersheds by implementation start year (panel b). The map shows the spatial coverage of priority areas across the Mississippi River Basin, while the bar chart highlights the number of subwatersheds that entered implementation in each year.

In high-yield regions such as the U.S. Midwest, excess nutrients often run off into surface water or leach into groundwater during rainfall, driving eutrophication and water-quality degradation. Nutrient pollution leads to oxygen-depleted "dead zones,"⁵ and imposes large social costs exceeding \$4.6 billion annually through damages to fishery, recreation, and property values (Kudela et al., 2015). High nitrate levels in drinking water also pose health risks, particularly for rural households relying on private wells (Ward et al., 2018).

Cover cropping, the practice of planting crops during off-seasons to protect soil, is increasingly recognized for its multifaceted benefits. The USDA underscores its vital role in soil erosion control, soil health improvement, water quality enhancement, and climate change adaptation and mitigation (Blanco-Canqui, 2018; Dabney et al., 2001; Fageria et al., 2005; Kaye and Quemada, 2017; Sarrantonio and Gallandt, 2003; Tonitto et al., 2006; Chen et al.,

⁵A "dead zone" is an area of low dissolved oxygen in aquatic systems where most marine life cannot survive. For instance, in the Gulf of Mexico, it forms each summer as nutrient runoff from the Mississippi River fuels algal blooms whose decomposition depletes oxygen in bottom waters.

2022).

Despite these documented environmental benefits, cover crop adoption remains limited because the private returns are often low or negative, particularly during the initial years of adoption. Establishment costs, short-term yield losses, and delayed soil fertility gains, as well as limited incentives for tenant farmers, make the practice financially unattractive without cost-share payments ([Bergtold et al., 2019](#); [Roesch-McNally et al., 2018](#); [Sawadgo et al., 2021](#)). These constraints justify policy interventions such as EQIP that aim to internalize the environmental externalities of cover cropping. This paper empirically examines the impact of EQIP–MRBI on cover crop adoption using an event study design (Section 4).

Cover crops reduce nutrient losses by limiting surface runoff and taking up nutrients in the short run while improving soil structure, water retention, and nutrient storage in the long term ([Blanco-Canqui, 2018](#); [Abdalla et al., 2019](#)). However, short-term effects on soluble nutrients can vary depending on residue decomposition and management practices ([Cober et al., 2018](#)). This paper empirically examines whether cover crops improve downstream nitrogen and phosphorus outcomes in the U.S. Midwest (Section 5).

Additional background on nutrient pollution, cover crop mechanisms, and private adoption incentives is provided in Appendix C.

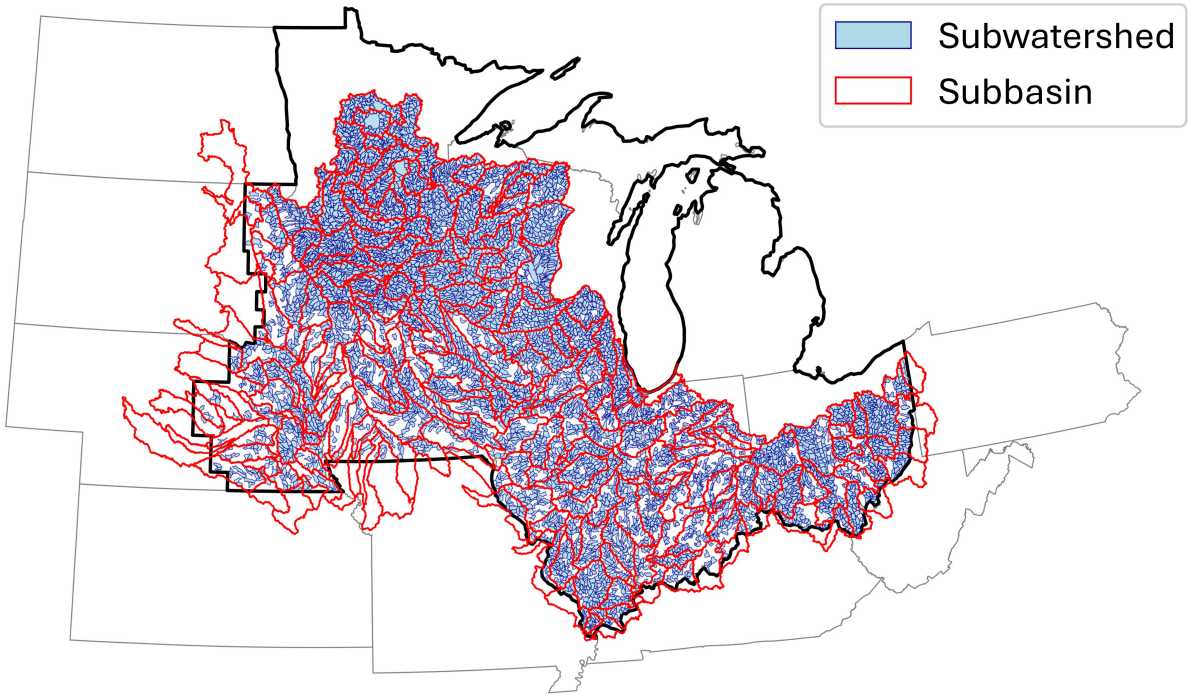
3 Data

We combine six sources of data for the analysis: (i) field-level cover crop adoption derived from satellite imagery (2007–2023), (ii) the universe of EQIP–MRBI implementation boundaries and timing, (iii) daily water quality monitoring data from the SNAPD (1980–2018), (iv) watershed boundaries and flow directions from the NHD, (v) land use from the USDA CDL and soil characteristics from the USDA gNATSGO, and (vi) weather data from the PRISM dataset. This section summarizes the key variables from each source. Additional details on data collection, variable construction, and dataset matching are provided in Appendix E.

Cover Crop Adoption. We construct field-level cover crop adoption data in corn and soybean fields in the 9 Midwest states in the U.S.⁶ from 2007 to 2023, leveraging remote sensing datasets and machine learning methods. The input data include Landsat-5, -7, and -8 imagery, more than 165,000 plot-year ground-truth labels, and auxiliary PRISM weather and USDA survey data. We classify cover crop adoption from satellite imagery using an ensemble machine-learning model. The model predicts cover crop adoption for more than

⁶The nine Midwestern states include Iowa, Indiana, Illinois, Ohio, Michigan, Minnesota, Wisconsin, and the eastern portions of North Dakota and South Dakota. These areas encompass eight of the nine states that have historically produced the most corn and soybeans.

Figure 2: Spatial Extent of the Data



Note: This figure shows the geographic scope of the study area. The black boundary indicates the region where field-level cover crop adoption data are available. Hydrologic units are represented at two nested scales: subwatersheds at the HUC-12 level (blue polygons) and subbasins at the HUC-8 level (red polygons). Each colored hydrologic unit shown in the figure contains at least one water quality monitoring station. The figure illustrates both the spatial coverage of the dataset and the definitions of hydrologic units used in the analysis.

3 million corn and soybean field-years, producing a binary indicator of cover crop presence during the off-season period (October 15–May 15). The spatial scope of the data is shown within the black boundary in Figure 2.

This dataset provides a reliable foundation for evaluating conservation program effectiveness and environmental outcomes. Our approach offers advantages over previous methodologies by drawing on a larger, more diverse dataset, incorporating advanced vegetation indices, enhancing data processing techniques, and leveraging ensemble models. The resulting dataset achieves an out-of-sample accuracy of 95.1%, correctly predicting labels for 95.1% of field-year observations in the test set. Because only 11% of observations are positives, a random classifier would attain a precision–recall area under the curve (PR-AUC) of 0.11; our model achieves 0.80, more than seven times higher. These results demonstrate that the model is accurate, robust, and well aligned with real-world agricultural practices.

Our algorithm to detecting cover crops improves upon [Seifert et al. \(2018\)](#) in four ways

(see Appendix D.1 for details). First, we use common land units (CLUs) to define field boundaries. Pixel-level variables are then aggregated to the field level, the smallest unit on which farmers make management decisions. This ensures consistency between the input data and the unit of analysis, rather than operating at the pixel level.

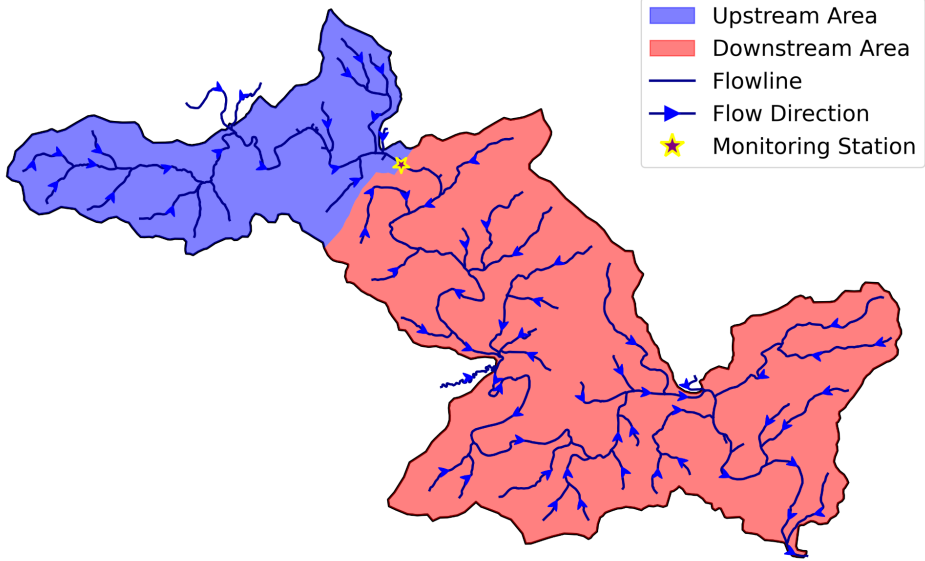
Second, we employ ground truth data from Land Core⁷, which includes over 165,000 field-year observations windshield observations collected from 2014 to 2019 across Indiana. These observations are randomly selected rather than limited to large homogeneous farms cooperating with the university. This broader and more diverse dataset ensures that our model is trained on a representative sample of the entire region, enhancing its ability to generalize across different types of fields and farming practices. In contrast, the previous study that relied on around 20,000 pixels from around 2,000 field-year observations for model training may have been limited by smaller, less diverse datasets, potentially leading to bias and overfitting problems. Another advantage of using windshield observations as ground-truth data is that they capture only fields with visibly established cover crops, in contrast to self-reported survey data where farmers may indicate intentions to plant cover crops but fail to achieve visible establishment due to weather or technical constraints. Because well-established cover crops are the most effective in reducing negative environmental impacts, this measure is particularly well-suited to the objectives of our study.

Third, we include a wider range of vegetation indices aside from the original variables included in Seifert et al. (2018), for example, the modified soil-adjusted vegetation index (MSAVI) and its later revision, MSAVI2 (Qi et al. 1994). These soil-adjusted indices address some limitations of the normalized difference vegetation index (NDVI) when applied to areas with a high degree of exposed soil surfaces. Using modified version of vegetation indices like MSAVI and MSAVI2 allows our model to better differentiate between crops and non-crop elements in challenging environments, leading to more accurate classifications. Furthermore, we interpolate vegetation indices to a weekly frequency to enhance the temporal resolution of the dataset, providing a more detailed representation of crop growth cycles and improving the model’s ability to identify cover crops. We also detect peaks and troughs in these time series to compute the integral of vegetation indices during the offseason, thereby extracting additional signals that would otherwise be missed.

Fourth, the final model is an ensemble of a Convolutional Neural Network–Long Short-Term Memory (CNN–LSTM) model, a Bidirectional Long Short-Term Memory (BiLSTM) model, and a random forest, which provide complementary strengths for prediction. The

⁷Ground-truth data were provided by Land Core, a 501(c)(3) nonprofit organization whose mission is to advance soil health policies and programs that create value for farmers, businesses, and communities (see <https://landcore.org>).

Figure 3: Upstream and Downstream Area Definition within a HUC-12 Subwatershed



Note: The figure illustrates how upstream and downstream areas are defined for each water-quality monitoring station using a representative subwatershed. The upstream (blue) and downstream (red) zones are delineated based on hydrological flowlines and direction, with the monitoring station (yellow star) serving as the reference point. The upstream cover crop adoption share for station i in year t is calculated as the ratio of acres with cover crops to total corn and soybean acres within the upstream area, as shown in the accompanying formula (1).

CNN–LSTM and BiLSTM models capture spatial and temporal dynamics in satellite imagery, while the random forest model effectively handles nonlinear relationships and reduces overfitting. Combining these models through an ensemble yields more stable and accurate predictions than any single model alone.

With this field-level cover crop adoption data, we first aggregate it to cover crop share and acreage to subwatersheds level for our analysis in Section 4. We then construct the key explanatory variable in Section 5, the cover crop adoption share upstream of the water monitoring station. It is defined as the ratio of the acreage of fields planted with cover crops during the off season to the total acreage of corn or soybean fields located upstream of the monitoring station within the same subwatershed as the station.

$$CC_{i,t}^{\text{up}} = \frac{\text{Acres with cover crops upstream of station } i \text{ in year } t}{\text{Total corn/soybean acres upstream of station } i \text{ in year } t} \quad (1)$$

Similarly, the downstream cover crop adoption is computed in the same manner. The boundaries of the upstream and downstream areas are illustrated in Figure 3.

Water Quality. We use the harmonized water quality data assembled by Krasovich

et al. (2022). This dataset synthesizes the Standardized Nitrogen and Phosphorus Dataset (SNAPD) by harmonizing 9.2 million monitoring readings from across the Mississippi and Atchafalaya River Basin (MARB). The SNAPD contains 4.8 million standardized observations of nitrogen and phosphorus compounds between 1980 and 2018, making it an unprecedented resource for understanding nutrient pollution in the region. From this raw dataset, we construct a monthly panel of multiple nutrient concentrations, including total nitrogen, total Kjeldahl nitrogen (TKN), nitrate, ammonia, total phosphorus, and orthophosphate. These variables serve as the core water quality outcomes for the analysis in Section 5.

Land Use. USDA Cropland Data Layer (CDL) is a crop-specific land cover data layer created annually for the continental U.S. using moderate resolution satellite imagery and extensive agricultural ground truth. The CDL has a ground resolution of 30 meters and has categorized each pixel into 254 different categories, including most crops grown in the U.S. and other common land coverage groups, such as forest, grassland, urban, and open water. We aggregated this data to monitoring station level by taking the ratio of each category of land use (e.g. cultivated, wetlands, forest, developed) to the total areas within 5 or 10 miles of the stations, or to the subwatershed boundaries to get total acreage of corn and soybean planted each year.

Weather. We use two sources of raster data: daily maximum and mean temperature, precipitation, and 30-year climate normals from the PRISM Climate Group at Oregon State University, and land cover data from the USDA Cropland Data Layer (CDL). The PRISM data are used in two parts of the analysis. In Section 4.3, we use 30-year climate normals to calculate the average length of the frozen season for each subwatershed and examine heterogeneity in program impacts across climatic zones. In Section 5, we construct weather variables within a 5-mile radius of each water monitoring station, including extreme degree days, growing degree days, and accumulated precipitation, to serve as control variables in the regression analysis. Appendix D.2 provides details on how the weather variables are constructed from the raw PRISM data.

Soil Characteristics. We extract soil characteristics from the gridded National Soil Survey Geographic Database (gNATSGO), a 30-m raster product integrating SSURGO and STATSGO2 data. Variables include plant-available water storage (AWS) and soil organic carbon stock (SOC) across multiple depth intervals, indices of droughtiness and rooting depth, crop productivity indices (NCCPI). For each farm plot, we compute spatial means to characterize soil water-holding capacity, fertility, and agronomic potential.

Summary Statistics Table 1 reports summary statistics for key variables used in the analysis. Panel A compares pre-treatment characteristics between EQIP–MRBI ever-treated and never-treated subwatersheds used in the analysis in Section 4. Both groups display broadly similar landscape and productivity features. On average, ever-treated subwatersheds have slightly larger average field sizes, higher cropland intensity, and modestly steeper slopes. These differences are consistent with the NRCS’s targeting of environmentally sensitive landscapes under MRBI. Baseline cover crop acreage and soil productivity index are similar across groups, suggesting broadly comparable pre-treatment adoption levels.

Panels B and C summarize cover crop adoption rates and nutrient pollution outcomes across monitoring locations in the Midwest used in the analysis in Section 5. On average, cover crops account for about 6% of corn and soybean fields, with substantial spatial variation. Some parts of the subwatersheds show almost no adoption, while others exceed 90 percent. Upstream and downstream adoption rates are similar. Nutrient pollution indicators exhibit substantial variability across monitoring sites. The mean total nitrogen (TN) concentration is about 3.9 mg/L, more than five times the EPA’s recommended reference range for the Midwest (0.3 – 0.8 mg/L), which indicates a high risk of eutrophication and biological impairment. Total Kjeldahl Nitrogen (TKN) measures the sum of organic nitrogen and ammonia, representing the pool of nitrogen that can later be transformed into nitrate—the most concerning form of nitrogen pollution for both water quality and human health. over time phosphorus (TP) and orthophosphate concentrations average around 0.2 mg/L, roughly twice the EPA’s 1986 ambient water quality criterion (0.1 mg/L). These elevated baseline nutrient levels highlight the importance of conservation programs such as EQIP–MRBI that target nutrient reductions.

4 Impacts of EQIP–MRBI Investments on Cover Crop Adoption

In this section, we evaluate the impacts of additional investments through EQIP–MRBI on cover crop adoption. Exploiting the dynamic timing of the EQIP–MRBI implementation across targeted subwatersheds within priority subbasins, we conduct event studies that compare subwatersheds eligible for MRBI funding to non-eligible subwatersheds located in the same priority zones. The focus is on examining the magnitude of additional cover crop adoption incentivized by the program, as well as the persistence of the program’s effects. We further examine heterogeneity in effects across climate conditions and states.

Table 1: Summary Statistics

Panel A. Balance of Pre-treatment Characteristics for Subwatersheds					
Variable	Ever-Treated		Never-Treated		p-value
	Mean	SE	Mean	SE	
Cover Crop Acreage	329.047	29.782	363.968	14.296	0.291
Cover Crop Share	0.052	0.007	0.075	0.004	0.005
Corn Share	0.334	0.010	0.312	0.004	0.047
Soybean Share	0.270	0.009	0.251	0.003	0.043
Average Field Size	45.005	1.371	41.944	0.495	0.037
Productivity Index (NCCPI)	0.752	0.006	0.750	0.003	0.720
Median Slope	1.638	0.079	1.445	0.029	0.023

Panel B. Cover Crop Adoption (CC)						
Variable	Count	Mean	Std. Dev.	Min	Median	Max
Upstream CC share	27,677	0.0593	0.1187	0	0.0129	0.9360
Downstream CC share	27,677	0.0614	0.1169	0	0.0159	0.9486
Upstream CC acreage	27,677	241.30	612.06	0	50.20	12,680.85
Downstream CC acreage	27,677	324.55	706.15	0	87.53	14,964.07

Panel C. Nutrient Pollution						
Variable	Count	Mean	Std. Dev.	Min	Median	Max
Total nitrogen	6,566	3.9073	3.5091	0.0644	2.7033	23.839
Total Kjeldahl nitrogen	71,562	1.0813	0.8510	0.02	0.8884	9.11
Nitrate	6,912	3.8213	4.2174	0.01	2	19.9
Ammonia	34,696	0.3180	0.4434	0.00232	0.1930	6.8
Total phosphorus	73,844	0.1823	0.2547	0.00656	0.1069	3.56
Orthophosphate	37,872	0.2023	0.2894	0.0031	0.1120	3.3

Note: This table reports summary statistics for key variables related to cover crop adoption and nutrient pollution in the U.S. Midwest. Panel A presents pre-treatment characteristics of subwatersheds, comparing EQIP-MRBI ever-treated subwatershed and never-treated subwatersheds. Variables include cover crop acreage and share in corn and soybean fields, corn and soybean shares in total subwatershed area, average field size, the NRCS productivity index (NCCPI), and median slope. Panels B and C summarize cover crop adoption and water quality outcomes, respectively. Cover crop variables represent the share and acreage of cover crops in upstream and downstream areas for each monitoring station within its HUC-12 subwatershed. Nutrient pollution variables include total nitrogen (TN), total Kjeldahl nitrogen (TKN, organic N and ammonia), nitrate, ammonia, total phosphorus (TP), and orthophosphate concentrations. Nutrient concentrations are expressed in milligrams per liter (mg/L).

4.1 Empirical Strategy

We conduct event studies that leverage the dynamic timing of the EQIP–MRBI implementation and its targeting policy in the top six Midwest states, including Minnesota, Wisconsin, Iowa, Illinois, Indiana, and Ohio. We treat the subwatersheds that were ever selected to receive extra funding through EQIP–MRBI as the treated units (shown in red in Figure 4), and the nearby subwatersheds within the same subbasin-level priority zone pre-designated by the federal level USDA NRCS, but not eligible for the additional MRBI funding, as the control units (shown in blue in Figure 4). We exclude subwatersheds that ever received treatment under the National Water Quality Initiative⁸ and those that do not intersect with the state in which the treated subwatersheds are located from our sample.

To evaluate the dynamic impacts of EQIP–MRBI on cover crop adoption, we implement an event study design following the framework of [de Chaisemartin and D'Haultfœuille \(2024\)](#). This approach is well-suited for policies such as EQIP–MRBI, where treatment is not necessarily absorbing: subwatersheds may switch in and out of treatment, and outcomes may depend not only on contemporaneous treatment status but also on past treatment exposure.

A standard two-way fixed effects event study can be biased when treatment effects vary across groups or when treatment status changes over time. In our setting, watersheds do not remain permanently treated after MRBI implementation; treatment can switch on and off across years. For this reason, we use the difference-in-differences estimator proposed by [de Chaisemartin and D'Haultfœuille \(2024\)](#), which is specifically designed for intertemporal treatments that may start, stop, or vary in intensity. The estimator compares outcome changes for switchers—units that change treatment status in a given year—to those of units with the same baseline treatment status that have not yet switched, under the assumptions of no anticipation and parallel trends across groups with identical prior treatment histories. This approach avoids the negative weighting and potential sign reversals that can arise in conventional two-way fixed effects, while providing consistent estimates of dynamic treatment effects in contexts with staggered and reversible treatment exposure.

The key building block is the group-by-period effect, defined as

$$\delta_{g,\ell} = \mathbb{E}[Y_{g,F_g-1+\ell} - Y_{g,F_g-1+\ell}(0, \dots, 0) \mid D], \quad (2)$$

⁸The National Water Quality Initiative (NWQI), launched in 2012, is another targeted sub-initiative of EQIP that provides additional financial and technical assistance to address critical water-quality concerns in priority watersheds nationwide. While MRBI focuses on nutrient reduction within the Mississippi River Basin, NWQI extends similar funding mechanisms to other high-priority areas across the country. Because some NWQI subwatersheds fall within MRBI's subbasin-level priority zones and only a small number are located in the six Midwestern states we analyze, we exclude NWQI subwatersheds to ensure that the estimated effects reflect MRBI-specific investments and are not confounded by overlapping conservation initiatives.

where g indexes subwatersheds, F_g denotes the year of the first treatment change in subwatershed g , and ℓ represents the number of periods relative to the first treatment change. The group-by-period effect is defined as the expectation of the difference between $Y_{g,F_g-1+\ell}$, the actual outcome, and the counterfactual outcome $Y_{g,F_g-1+\ell}(0, \dots, 0)$, which represents what would have occurred had the subwatershed remained untreated for ℓ additional periods. D is the treatment assignment design across groups and time.

Our target parameter for each period ℓ is the average of group-by-period effects across groups within each relative time period:

$$\delta_\ell = \frac{1}{N_\ell} \sum_{g:F_g-1+\ell \leq T_g} \delta_{g,\ell}, \quad (3)$$

where N_ℓ is the number of subwatersheds for which $\delta_{g,\ell}$ can be estimated at event time ℓ , and T_g is the final observed period for subwatershed g . These parameters capture how cover crop adoption evolves in the years before and after EQIP–MRBI rollout.

Identification relies on two standard conditions. First, in the absence of EQIP–MRBI, adoption trends would have been parallel across treated and not-yet-treated subwatersheds. Second, farmers do not systematically anticipate the policy; that is, there are no treatment-induced behavioral changes prior to program rollout.

For valid inference, we assume that outcomes across subwatersheds are independent conditional on the treatment design. Additionally, asymptotic restrictions and standard regularity conditions are required to ensure consistency and asymptotic normality of the estimators.

We set the baseline period, $\ell = 0$, as the reference period, representing the year immediately preceding the first MRBI treatment. Periods with negative event times ($\ell \in \{-1, -2, -3, -4\}$) serve as placebo estimators, comparing pre-treatment trends between subwatersheds that are about to receive MRBI funding and those not yet treated. These placebo coefficients provide a test of the parallel-trends assumption underlying the identification of causal effects. The post-treatment effects are estimated for event times $\ell = 1$ through $\ell = 11$, capturing both the contemporaneous and lagged responses in cover-crop adoption following EQIP–MRBI implementation.

Another parameter that we are estimating is the *average total effect per unit of treatment*, defined as

$$\delta = \frac{\sum_{g:F_g \leq T_g} \sum_{\ell=1}^{T_g-F_g+1} \delta_{g,\ell}}{\sum_{g:F_g \leq T_g} \sum_{\ell=1}^{T_g-F_g+1} D_{g,F_g-1+\ell}} \quad (4)$$

where T_g is the last period in which there remains at least one subwatershed that has not yet been treated. In our application, the treatment intensity in period ℓ after the first treatment, $D_{g,F_g-1+\ell}$, is a binary variable that equals to one when the subwatershed is

eligible for additional EQIP funding through MRBI and zero otherwise.

This parameter, δ , aggregates the dynamic treatment effects across both time and groups, dividing it by the total number of treatment-unit changes. Intuitively, it measures the sum of the impact of one year MRBI addditional investments through EQIP, both at the period when the treatment change occurs (the concurrent effect) and in all subsequent periods (the lagged effects), and then averages these cumulative effects across all ever-treated subwatersheds. From a policy perspective, δ is informative because it is a natural metric for cost-benefit and cost-effectiveness analyses, allowing us to assess whether the cumulative benefits of treatment in cover crop adoption justify the total program expenditures.

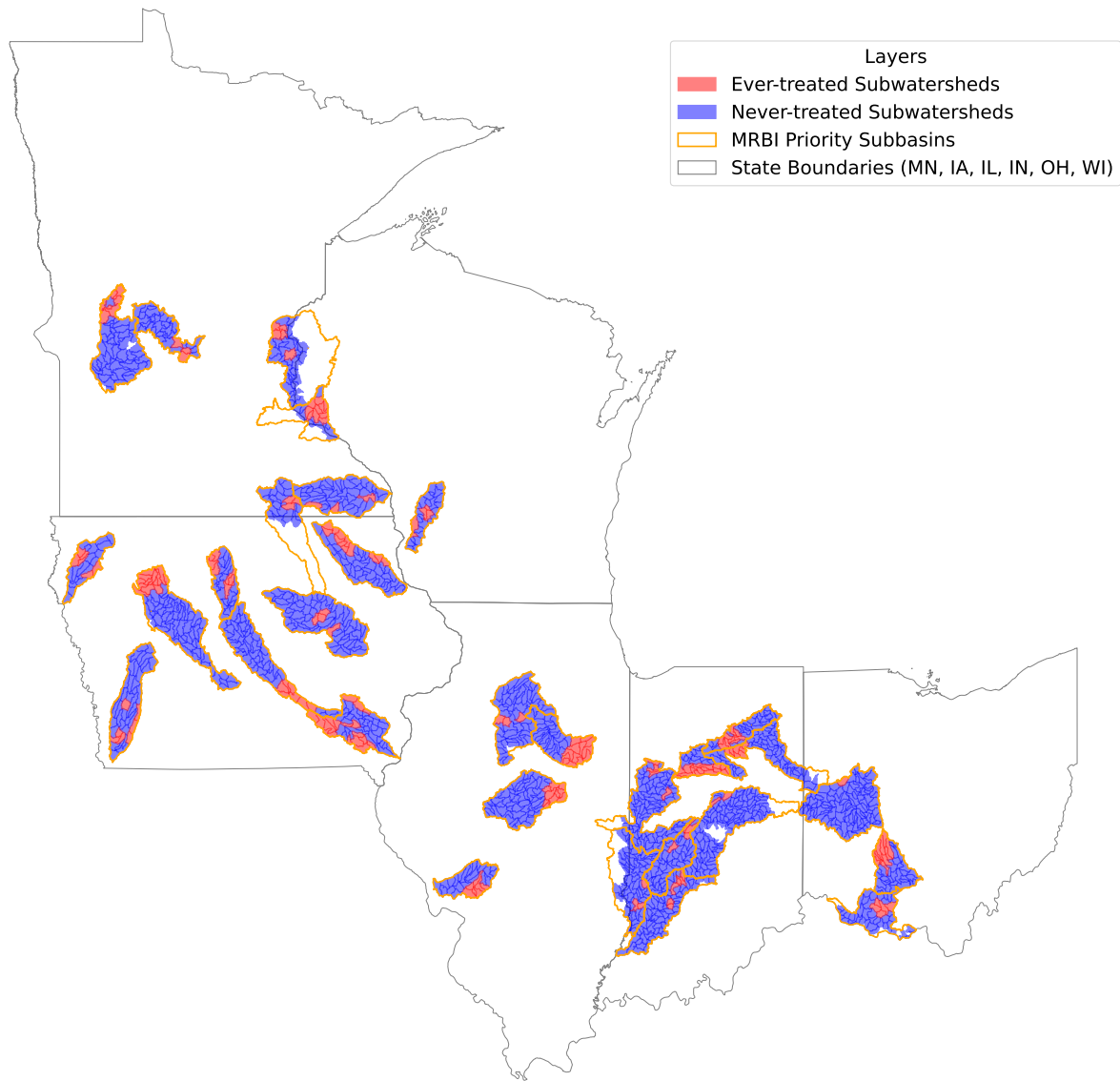
4.2 Results

The results corresponding to target parameter (3) are presented in Figure 5. The event-study estimates indicate that the treatment effects on cover crop adoption build gradually over time (Figure 5a). For cover crop share, although the effects are not statistically significant in the first and fourth years following program implementation, they become positive and statistically significant beginning in the second year, peaking in the ninth year with a 5.3 percentage point increase in treated subwatersheds relative to controls. This represents an 88% increase over the mean cover crop adoption rate of 6% at the peak. The joint test of effects from year 1 to year 11 strongly rejects the null hypothesis of no post-treatment effects ($p = 0.0018$). The effects build gradually over time because they capture the total impact—combining both the contemporaneous response to MRBI funding and the lagged effects of cumulative exposure to additional incentives over multiple years of implementation (typically three to five years).

Reassuringly, the placebo estimates to the left of the grey dashed line representing pre-trends provide support for the identifying assumptions. Pre-treatment coefficients are small in magnitude and statistically indistinguishable from zero, and the joint test of pre-trends fails to reject at conventional levels ($p = 0.28$). This pattern suggests that treated and untreated units followed parallel trajectories before the intervention and that anticipation effects are unlikely.

The average total effect on cover crop adoption share from one additional year of investment through EQIP–MRBI is 1.75 percentage points (95% confidence interval: [0.64, 2.87]) increase from a baseline mean of 6%, representing a 29% increase that is both economically and statistically significant. This estimate reflects the total effect, combining both the contemporaneous and lagged impacts of one year of EQIP–MRBI treatment, averaged across all ever-treated subwatersheds. We use this estimate as the basis for the subsequent

Figure 4: EQIP–MRBI Priority Subbasins and Subwatershed Treatment, 2012–2023



Note: This map shows the geographic distribution of Mississippi River Basin Initiative (MRBI) priority areas in the Upper Midwest. State boundaries (gray) include Minnesota, Iowa, Illinois, Indiana, Ohio, and Wisconsin. MRBI, a subinitiative of the Environmental Quality Incentives Program (EQIP), designates priority subbasins (HUC-8) through the federal NRCS; these are outlined in orange. Within these, HUC-12 subwatersheds that were ever treated under MRBI between 2012 (the first treated cohort) and 2023 (the end of the data) are shown in red, while never-treated subwatersheds are shown in blue. Subwatersheds that ever received treatment under the National Water Quality Initiative (NWQI) are excluded, as are subwatersheds not intersecting with the state in which the treated subwatersheds are located.

cost–benefit analysis.

The results using cover crop adoption acreage as outcome show similar patterns in Figure 5b. While the effects are not statistically significant in the first 3 years after implementation, they become positive and statistically significant from years 4 to 8, also peaking in year 9 at 362 acres, though the estimate is imprecise after year 9. The average total effect from one year of MRBI treatment is 157 acres (95% confidence interval: [49.48, 264.74]). The test of joint nullity of the placebos fails to reject at conventional levels ($p=0.24$).

Two key dimensions of the effectiveness of PES programs are additionality and persistence. A cover-cropped acre is *additional* if the conservation action is induced by the EQIP–MRBI incentive rather than something the farmer would have undertaken in the absence of the program. When EQIP payments go to farmers who would have adopted cover crops regardless of the incentive, the payment becomes a pure transfer, generating no additional environmental benefit and imposing a cost on taxpayers. Only additional conservation produces real, incremental environmental improvements.

The average treatment effects from our event study capture the additional adoption of cover crops induced by EQIP–MRBI funding. Because the event-study design compares treated subwatersheds to those not yet treated, which serve as a proxy for the counterfactual under the parallel-trends assumption, the estimated effects represent the incremental cover crop adoption caused by the program rather than background adoption that would have occurred in its absence. Moreover, the outcome data are derived from satellite imagery, which measure total adoption on the landscape, not only acreage enrolled in EQIP contracts.

We quantify additionality as the ratio between the total acreage of cover crops induced by one year of EQIP–MRBI funding and the acreage that could have been directly supported by that same amount of program funding. Consider an average subwatershed receiving \$37,682 in additional EQIP–MRBI support, which corresponds to roughly 791 acres of cover crops that could be funded⁹. The estimated total effect of 157 acres of additional cover crop adoption thus implies an additionality rate of $\frac{157}{791} \approx 19.9\%$ (95% confidence interval: [6.3%, 33.5%]). Even when evaluated at the peak year, considering that farmers are learning how to grow cover crops correctly in the first few years, the additionality rate remains modest, at about 46%.

Adoption is *persistent* if the farmer continues to plant cover crops after program funding ends. Without persistence, temporary financial incentives may yield only short-lived behavioral changes. For practices like cover cropping, discontinuation can quickly reverse prior environmental gains: soil health improvements deteriorate, sequestered carbon is released back into the atmosphere, and water-quality benefits diminish once the practice stops.

⁹Calculated by dividing \$37,682 by the median EQIP payment rate of \$47.64 per acre.

Therefore, persistence determines the long-term effectiveness of conservation policy.

For EQIP–MRBI, treatment spells typically last three to five years, and each EQIP cover crop contract extends up to five years. Accordingly, the first nine event-time coefficients capture the dynamic effects during active funding, while periods ten and eleven reflect post-treatment dynamics. These latter estimates indicate whether the impacts of earlier MRBI investments in cover crops persist, fade, or reverse once program funding ends. As shown in Figure 5a, the effects remain positive and statistically significant in years 10 and 11 after treatment implementation starts. We quantify persistence as the ratio between the average effects in years 10–11 and the effect in year 9, which gives us 77.5% (95% confidence interval: [19.2%, 135.8%]). This implies substantial persistence in EQIP-induced cover crop adoption. This contrasts with the conventional evidence in the literature, which generally emphasizes high disadoption rates of cover crops though in other context(e.g., Pathak et al., 2024; Plastina et al., 2024). Our finding of persistence after EQIP contracts expire suggests that private benefits may in fact be stronger than previously thought. This result also aligns with the low additionality we estimate.

4.3 Heterogeneous Effects

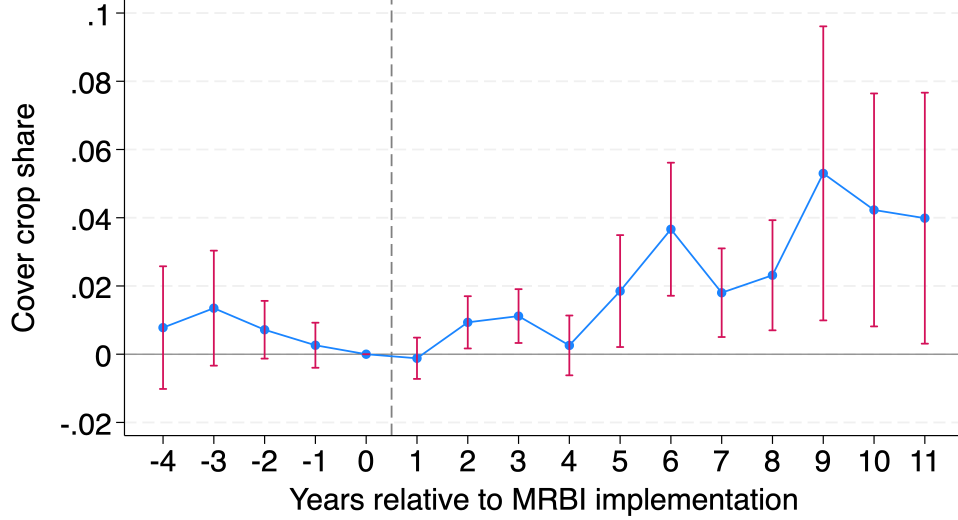
We conduct event-study analyses separately for subwatersheds with different lengths of the cover crop growing season. Using 30-year climate normal data, we divide the sample into two groups: (a) the top 50% of subwatersheds with shorter frozen seasons and (b) the bottom 50% with longer frozen seasons. In group (a), the average frozen period is 65 days, whereas in group (b) it is 112 days, where there is a difference of nearly two months in the potential growing window for cover crops.

The results in Figure A2 highlight stark heterogeneity. For group (a), the average total effect of EQIP–MRBI is an increase of 3.53 percentage points in cover crop adoption (95% confidence interval: [2.21, 4.85]). These effects persist beyond the funding period: from year 2 to year 11 after treatment initiation, all estimated impacts are statistically significant and positive. By contrast, in group (b), the average total effect is statistically indistinguishable from zero at -0.08 (95% confidence interval: [-0.97, 0.82]). Moreover, starting in year 9, the estimates turn negative and statistically significant, suggesting a decline in adoption relative to baseline.

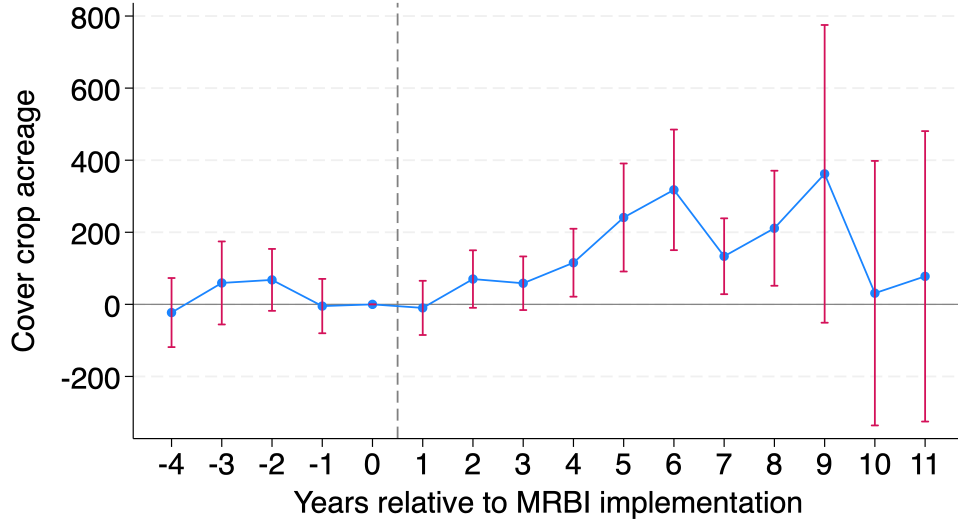
Two mechanisms may explain this pattern. First, the allocation of funding in shorter growing-window regions appears non-additional, with subsidies failing to generate sustained increases in adoption. Second, farmers may initially attempt cover cropping with support from subsidies but subsequently disadopt when faced with implementation challenges—such

Figure 5: Effects of MRBI on Cover Crop Adoption

(a) Cover Crop Share



(b) Cover Crop Acreage



Note: The figure presents estimates from a difference-in-differences event-study design in Equation (3) [de Chaisemartin and D'Haultfoeuille \(2024\)](#). Panel (a) reports results using cover crop adoption acreage as the outcome, while panel (b) uses the adoption share. All coefficients are estimates relative to the baseline year immediately preceding project implementation ($t=0$). The horizontal line at 0 marks this baseline, and the vertical dashed grey line corresponds to the year of MRBI initiative implementation. Standard errors are clustered at the HUC-12 level. Red bars indicate 95% confidence intervals. The analysis uses an unbalanced panel of HUC-12 watersheds from 2008–2023, consisting of 209 ever-treated HUC-12s and 1,262 never-treated controls, for a total of 16,803 HUC12–year observations and 1,064 treatment switch periods.

as reduced yields or higher costs in areas with short growing windows. In fact, the estimates suggest that farmers in these regions eventually adopt cover crops at rates below their pre-treatment baseline, pointing to a discouragement effect.

These findings underscore the importance of targeting conservation programs toward areas with more favorable climate conditions and longer growing windows, where cover crops are more likely to be viable and policy support can generate persistent environmental benefits.

We also explore heterogeneity in program effects across states, recognizing that state-level discretion in EQIP–MRBI implementation could lead to differential outcomes. These exploratory results are presented in Appendix E (Figures A9 and A8) and should be interpreted as descriptive patterns rather than causal estimates.

5 Impacts of Cover Crop Adoption on Water Pollution

To evaluate the impact of cover crops on ambient surface water pollution, we conduct a panel data analysis examining the concentrations of multiple nutrient pollutants in relation to upstream cover crop adoption. This approach allows us to estimate the causal effect of cover crops on water quality and to identify the mechanisms underlying this effect.

5.1 Empirical Strategy

We first regress the log of the pollutant concentration on upstream cover crop adoption share as in Equation (5).

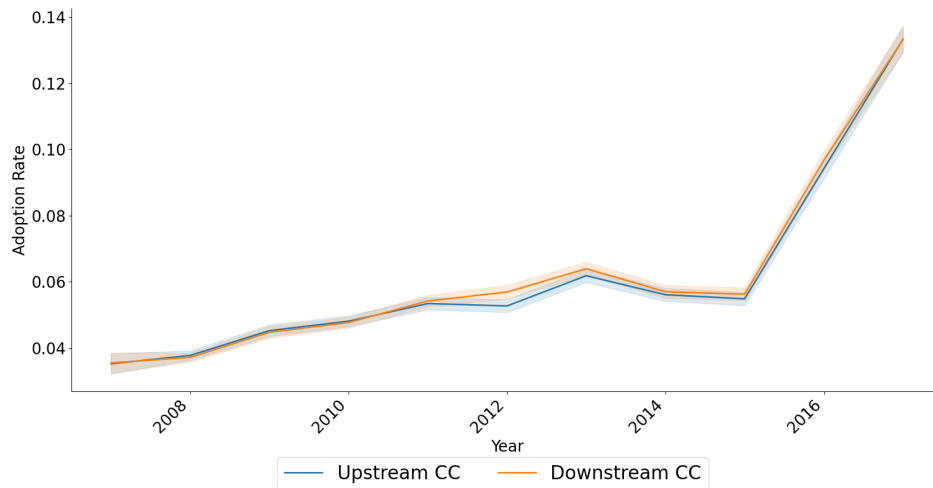
$$\ln(Y_{ihym}) = \beta_0 + \beta_1 CC_{ihy}^{up} + \alpha_{hy} + \mu_m + \varepsilon_{ihym} \quad (5)$$

where i denotes the index for the water quality monitoring station, h represents the subwatershed, y indicates the year, and m refers to the month. The dependent variable, Y_{ihym} , captures the monthly average concentration of a specific nitrogen or phosphorus compound at the station level. The key explanatory variable, CC_{ihym}^{up} , represents the upstream cover crop adoption share. Month fixed effects, μ_m , account for seasonality, while subwatershed-by-year fixed effects, α_{hy} , control for time-varying changes in watershed-targeting policies.

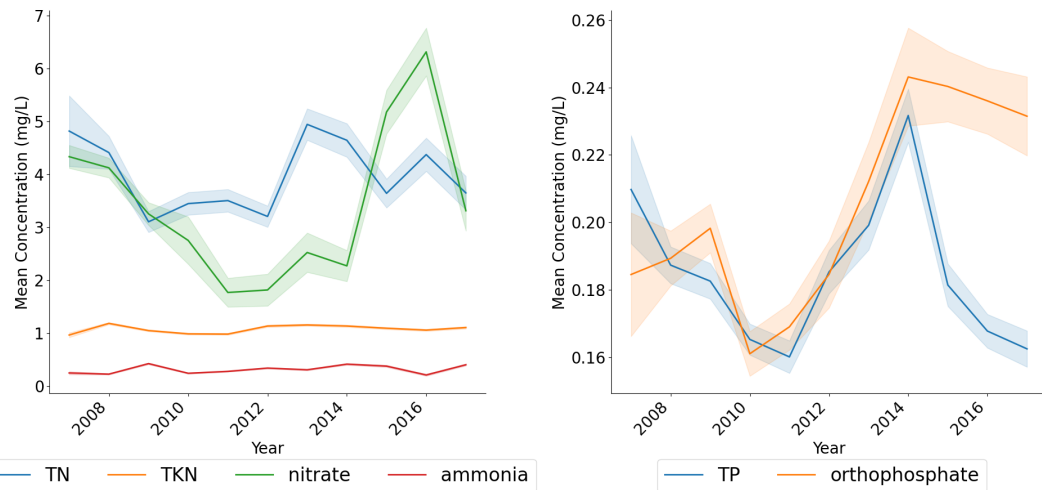
We then run a placebo test with the downstream cover crop adoption share as the placebo and also include other control variables like weather variables, cash crops in the area, and urban development.

$$\ln(Y_{ihym}) = \beta_0 + \beta_1 CC_{ihy}^{up} + \beta_2 CC_{ihy}^{down} + \mathbf{X}_{ihym}\gamma + \alpha_{hy} + \mu_m + \varepsilon_{ihym} \quad (6)$$

Figure 6: Overview of Key Variables



(a) Trends in Cover Crop Adoption Over Time



(b) Nitrogen Compound Concentration

(c) Phosphorus Compound Concentration

Note: The figure summarizes temporal patterns in cover crop adoption and nutrient concentrations, showing a sharp rise in adoption after 2016 alongside substantial variation in nitrogen and phosphorus compound concentrations across years. Panel (a) shows the average cover crop adoption rate over time for upstream and downstream areas of each water monitoring station, illustrating a steady increase in adoption since 2008 and a sharp rise after 2016. Panel (b) plots the mean concentrations of nitrogen compounds—total nitrogen (TN), total Kjeldahl nitrogen (TKN, organic N and ammonia), nitrate, and ammonia—revealing substantial interannual variability and generally higher fluctuations in nitrate concentrations relative to organic and ammonia nitrogen. Panel (c) presents trends in phosphorus compounds, including total phosphorus (TP) and orthophosphate, which exhibit similar temporal patterns with a notable increase around 2014 followed by a decline. Shaded bands represent 95% confidence intervals around annual means.

Downstream cover crop adoption share serves as a placebo because cover crops downstream of the monitoring station could not possibly affect the surface water quality reading at the station. At the same time, the downstream area immediately neighbors the cover crops in the upstream area, exposing both to similar environmental and socio-economic conditions. If there exist unobserved local factors within a subwatershed and year that influence water quality at the monitoring station but are not absorbed by the subwatershed-by-year fixed effect (e.g., environmental organizations promoting conservation practices or broader social pressures to adopt them), then downstream cover crop adoption may also be correlated with pollutant concentrations at the monitoring station. In that case, the estimated coefficient $\hat{\beta}_2$ would appear statistically significant. We therefore conduct a placebo test using downstream cover crop adoption share: if there is no unobserved heterogeneity in the error term that jointly affects both water quality and downstream cover crop adoption within a subwatershed and year, then the coefficient on downstream cover crop adoption share should be statistically insignificant. Figure 6a displays time trends in cover crop adoption shares. There is minimal difference between the mean cover crop adoption share in the upstream and downstream areas. This similarity provides descriptive support for using downstream cover crop adoption as a valid placebo for the upstream measure.

A first set of control variables in vector \mathbf{X}_{ihym} are weather factors, including growing degree days (GDD), extreme degree days (EDD), mean precipitation, and mean precipitation squared, recognizing the relationship between rainfall characteristics and the role of cover crops in mitigating soil erosion ([Blanco-Canqui, 2018](#)). Additional controls include the proportion of land under soybean cultivation within a 5-mile radius of the monitoring station and the proportion of developed area within a 10-mile radius. These controls address potential omitted variable bias, as crop choice, land use, and future urbanization expectations are possibly correlated with the adoption of conservation practices.

The identification assumptions for this analysis are twofold. First, we assume that the direction of water flow is exogenous and independent of cover crop adoption, conditional on the control variables, subwatershed-by-year fixed effects, and month fixed effects. Second, we assume that, conditional on the cover crop adoption share near a monitoring station, the adoption status of individual fields nearby is exogenous when accounting for the control variables and fixed effects. Specifically, this assumption does not preclude selection patterns where fields adopting cover crops are located near areas with higher baseline levels of water pollution. Instead, it asserts that, given the total acreage of cover crop adoption within a subwatershed, the spatial distribution of adopting fields is exogenous with respect to the location of the water quality monitoring station.

5.2 Results

The results are presented in Tables 2 and 3. Column (1) in Table 2 shows that a one percentage point increase in upstream cover crop adoption share leads to a 0.83% decrease in total nitrogen concentration in ambient surface water. The effect remains both statistically significant and stable in magnitude after including downstream cover crop adoption share as a placebo and adding control variables as in column (2). At an average upstream cover crop adoption share of 6% in our sample, the estimated elasticity suggests economically meaningful water-quality improvements from marginal increases in adoption. While a linear extrapolation implies large potential reductions in total nitrogen, such interpretation should be treated as illustrative given the observed range.

When examining specific nitrogen compounds, column (4) indicates that a one percentage point increase in upstream cover crop adoption share reduces total Kjeldahl nitrogen (TKN), which includes organic nitrogen and ammonia, by 0.43%, suggesting that roughly half of the total nitrogen reduction comes from these compounds. However, columns (6) and (8) show no statistically significant effect on nitrate and ammonia, the two most crucial soluble nitrogen compounds.

These findings align with biological and agronomic literature, which suggests that cover crops reduce sediment-bound organic nitrogen runoff by decreasing peak water flow and delaying runoff initiation during precipitation events. However, evidence on soluble nitrogen compounds remains mixed. While cover crops can absorb excess soil nitrogen, it can also accelerate decomposition, and certain cover crop species can fix atmospheric nitrogen, potentially increasing soluble nitrogen levels in the soil and making them more susceptible to runoff.

Our finding that a one-percentage-point increase in cover crop adoption share leads to a 0.83% reduction in total nitrogen is somewhat smaller than the effect reported by [Hsieh and Gramig \(2024\)](#), who found that a one-percentage-point increase in cover crop adoption was associated with a 0.06 mg/L (or roughly 2%) reduction in total nitrogen. Their estimate is approximately twice as large as ours and is based on analysis at the subbasin level, which aggregates two levels above the subwatershed. This higher level of aggregation may increase the risk of omitted variable bias, as it does not fully account for local heterogeneity or policy targeting effects. Compared to [Liu et al. \(2023\)](#), who reported a 0.29% total nitrogen reduction associated with a 10% increase in EQIP payments at the national watershed scale, our estimate is four times larger. This difference may reflect the fact that [Liu et al. \(2023\)](#) aggregated across all EQIP-eligible practices, many of which are not directly aimed at nutrient reduction, and that their analysis at the watershed level is also more vulnerable

to omitted variable bias due to federal and state targeting policies. [Hanrahan et al. \(2021\)](#), using small-scale edge-of-field experiments, found much larger effects, with cover crop fields reducing total nitrogen in tile drainage by 52% and in surface runoff by 6%. Overall, our estimate provides a more accurate and targeted assessment of cover crop impacts on nitrogen outcomes, bridging the gap between small-scale experimental evidence and coarse observational estimates and offering credible evidence at the subwatershed scale.

Column (2) of Table 3 shows no statistically significant effect of cover crop adoption on total phosphorus concentration. Because phosphorus is often bound to soil particles and moves with sediment rather than in dissolved form, short-term changes at the monthly scale are less apparent than for nitrogen.

However, a caveat exists: a one percentage point increase in cover crop adoption share raises orthophosphate concentration by 0.53%, as shown in column (4). Orthophosphate is a soluble form of phosphorus readily taken up by aquatic plants and algae, whereas most phosphorus in aquatic systems exists in particulate or organic forms that are less bioavailable. Since phosphorus is often the limiting nutrient in freshwater ecosystems, an increase in orthophosphate could accelerate eutrophication and heighten algal bloom risks.

Table 2: Effects of Cover Crop Adoption on Nitrogen Compound Concentrations

Dependent Variables:	ln(total nitrogen)	ln(organic N + ammonia)	ln(nitrate)	ln(ammonia)				
	(1)	(2)	(3)	(4)	(5)	(6)	(7)	(8)
Cover Crop Upstream	-0.828*** (0.257)	-0.877** (0.375)	-0.345*** (0.131)	-0.429** (0.169)	-1.121 (1.244)	-0.678 (1.467)	0.233 (0.319)	0.354 (0.330)
Cover Crop Downstream		0.074 (0.817)		-0.262 (0.283)		0.269 (2.013)		0.393 (0.737)
Control Variables		✓		✓		✓		✓
Subwatershed-Year FE	✓	✓	✓	✓	✓	✓	✓	✓
Month FE	✓	✓	✓	✓	✓	✓	✓	✓
Observations	6,566	6,566	71,562	71,562	6,912	6,912	34,696	34,696
R ²	0.730	0.734	0.564	0.572	0.780	0.783	0.421	0.424

Notes: This table presents the estimated effects of upstream CC adoption on various water pollution indicators. The dependent variables include the natural logarithm of total nitrogen (TN), total Kjeldahl nitrogen (TKN, organic nitrogen and ammonia), nitrate, and ammonia concentrations in water. Every two columns correspond to a different dependent variable. Standard errors clustered at the subbasin level are reported in parentheses. The control variables include growing degree days (GDD), extreme degree days (EDD), mean precipitation, mean precipitation squared, the proportion of land growing soybean/corn within a 5-mile radius of the water monitoring station, and the proportion of developed area within a 10-mile radius of the water monitoring station. All models include subwatershed-by-year and month fixed effects. The sample period spans from 2007 to 2017. Statistical significance is denoted by ***: $p < 0.01$, **: $p < 0.05$, and *: $p < 0.1$.

Our null finding on the effect of cover crops on total phosphorus contrasts with prior studies summarized in Table A2 but highlights important differences in scale and identification strategies. Liu et al. (2023) used an upstream-downstream difference-in-differences design but aggregated EQIP payment data at a higher level than the subwatershed, without fully controlling for policy and funding targeting. As a result, their finding that a 10% increase in EQIP payments is associated with a 0.23% increase in total phosphorus may partially reflect reverse causality, where areas with higher baseline phosphorus levels receive more conservation funding. Hanrahan et al. (2021), by contrast, relied on small-scale edge-of-field experiments in Ohio and found mixed effects, with cover cropped fields increasing dissolved reactive phosphorus (DRP) in tile drainage by 7% but reducing DRP in surface runoff by 16%. Compared to these studies, our analysis at the subwatershed scale, with controls for local targeting and upstream-downstream dynamics, finds no statistically significant effect of cover crop adoption on total phosphorus, suggesting that aggregate observational patterns and small-scale experimental results do not necessarily translate into detectable improvements in ambient water quality at the landscape scale.

Table 3: Effects of Cover Crop Adoption on Phosphorus Compound Concentrations

Dependent Variables:	ln(total phosphorus)	ln(orthophosphate)	
Cover Crop Upstream	0.050 (0.289)	0.153 (0.239)	0.322 (0.311)
Cover Crop Downstream		0.019 (0.667)	0.703 (0.602)
Control		✓	✓
Subwatershed-Year FE	✓	✓	✓
Month FE	✓	✓	✓
Observations	73,844	73,844	37,872
R ²	0.629	0.642	0.712
			0.719

Notes: This table presents the estimated effects of upstream CC adoption on various phosphorus pollution indicators. The dependent variables include the natural logarithm of total phosphorus (TP) and orthophosphate concentrations in water. Every two columns correspond to a different dependent variable. Standard errors clustered at the subbasin level are reported in parentheses. The control variables include growing degree days (GDD), extreme degree days (EDD), mean precipitation, mean precipitation squared, the proportion of land growing soybean/corn within a 5-mile radius of the water monitoring station, and the proportion of developed area within a 10-mile radius of the water monitoring station. All models include subwatershed-by-year and month fixed effects. The sample period spans from 2007 to 2017. Statistical significance is denoted by ***: p < 0.01, **: p < 0.05, and *: p < 0.1.

5.3 Monthly Effects of Cover Crops on Water Pollution

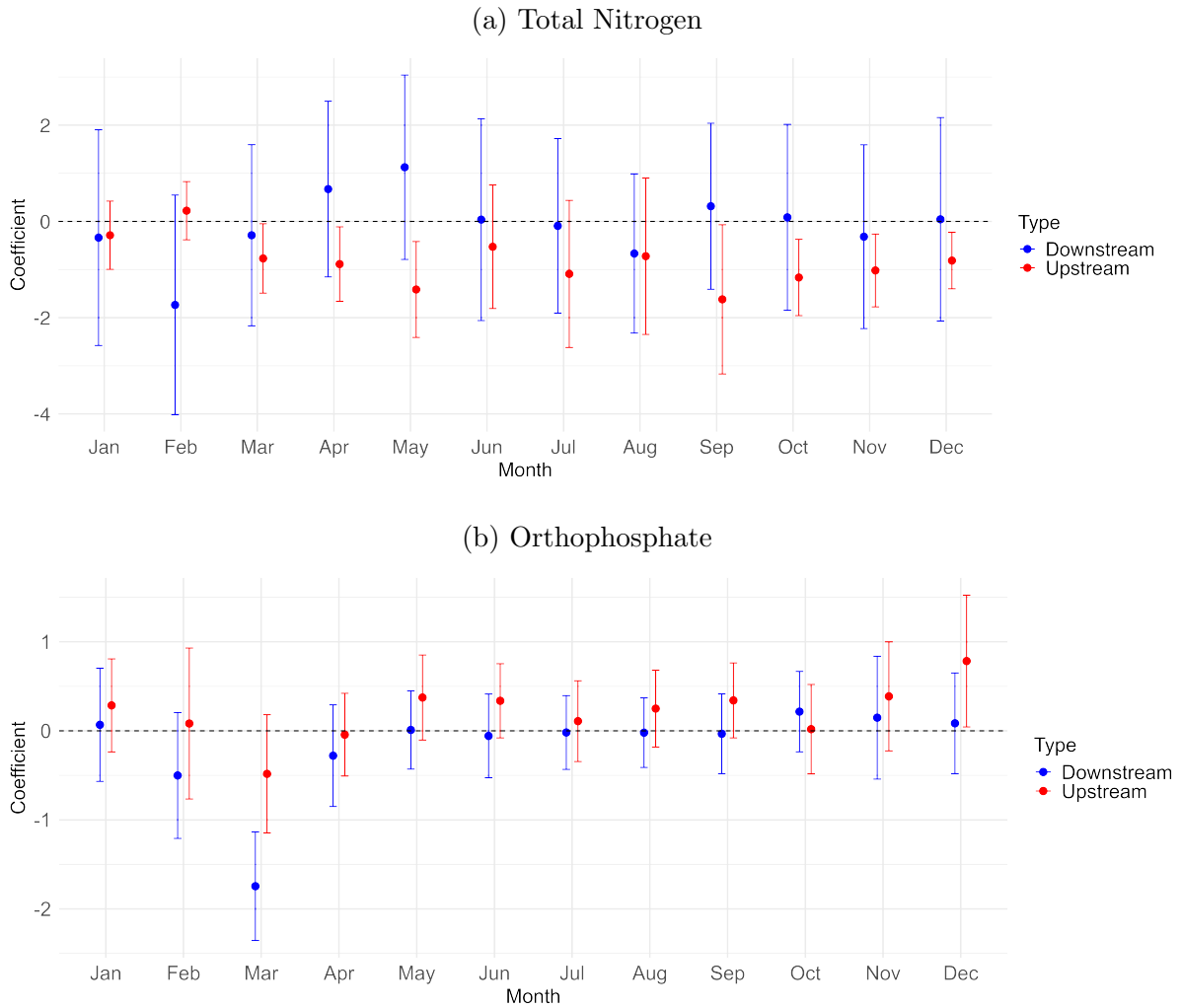
There is a potential concern that farmers may implement other water-related conservation practices alongside cover crops as part of a broader management strategy. To ensure that the observed effects are specifically attributable to cover crop adoption, we examine the month-specific impacts of cover crops on surface water quality. Our hypothesis is that if cover crop adoption drives the effects, the effects should be most pronounced between October and May, excluding periods when the ground is frozen. During this time, cover crops play a crucial role in preventing soil exposure and reducing runoff, as bare soil without cover crops would be more vulnerable to erosion and nutrient loss. However, when the ground is frozen, runoff is minimal, and cover crops cannot grow, so we do not expect to see statistically significant effects. To test this, we estimate the following regression model:

$$\ln(Y_{ihym}) = \beta_0 + \sum_{n=1}^{12} \mathbf{1}[m = n] \times (\beta_n CC_{ihym}^{up} + \gamma_n CC_{ihym}^{down}) + \mathbf{X}_{ihym}\gamma + \alpha_{hy} + \varepsilon_{ihym} \quad (7)$$

This regression model evaluates the month-specific effects of cover crop adoption on surface water quality at monitoring station i , located within subwatershed h , in year y and month m . The key independent variables include the upstream cover crop adoption share, CC_{ihym}^{up} , interacted with monthly indicator variables, $\mathbf{1}[m = n]$, allowing the effects to vary by month. The model follows the same structure as the primary specification in Section 5, with the only modification being the interaction with month indicators to isolate month-specific impacts. The coefficients β_n capture the marginal effect of upstream cover crop adoption in month n .

Figure 7 shows the estimated month-specific effects of upstream (red) and downstream (blue) cover crop adoption on total nitrogen (panel 7a) and orthophosphate (panel 7b) pollutants in surface water. The results suggest that upstream cover crop adoption lowers nitrogen pollution mainly in the fall and spring, when cover crops are actively growing and the soil is not frozen. This evidence aligns with the literature on cover crop impacts, as cover crops are most effective at nutrient retention when they can block sediments from running off and uptake excessive nitrogen from the soil before it leaches into waterways. In contrast, there are few effects contemporaneously during the cash crop growing season. The placebo test using downstream cover crop adoption (blue) does not present any systematic impact at the same time, further supporting the validity of the results. A similar seasonal pattern emerges for orthophosphate, where we observe a December increase that likely reflects nutrient release during cover crop decomposition.

Figure 7: Effects of Upstream and Downstream Cover Crop Adoption on Surface Water Quality Outcomes by Month



Note: This figure shows coefficients on upstream and downstream cover crop adoption share by month from regressions in equation (7) that control for precipitation, growing degree days, extreme degree days, and the shares of cash crops and urban development in the area. Dots represent estimated coefficients, and dashed lines indicate 95% confidence intervals. Upstream cover crop adoption (red) is expected to influence water quality, while downstream adoption (blue) serves as a placebo test. Data covers years 2007 to 2017. Standard errors are clustered at the subbasin level.

5.4 Robustness Checks

We conduct a series of robustness checks to assess the sensitivity of our results to alternative specifications, as reported in Table A3. Specifically, we re-estimate the models using daily data instead of monthly averages and introduce additional fixed effects, including year-by-month interactions and day-of-year controls, to better capture seasonality and temporal variation. We also test the inclusion of control variables, placebo variables, and minimum observation thresholds per site. Across all specifications, the estimated effects of upstream cover crop adoption on nitrogen outcomes remain consistently negative and statistically significant, with effect sizes similar to or even larger than those obtained using the baseline monthly models. These findings reinforce the robustness of our main results and strengthen confidence that the estimated reductions in nitrogen pollution are not driven by modeling choices or data aggregation.

6 Cost–Benefit Analysis of EQIP–MRBI Investments

We define the benefit–cost ratio (BCR) as the average dollar value of reduced nitrogen damages, based on the causal impact of cover crops on water quality in each subwatershed, divided by the total EQIP–MRBI expenditure in that subwatershed. Specifically, this measure accounts for additionality by including only the 20% of cover crop acreage that is attributable to the subsidy. Specifically, we use the following formula to calculate the BCR of EQIP–MRBI:

$$\text{BCR} = \frac{\hat{\delta}_{\text{MRBI}}^{\text{CC}} \times \hat{\beta}_{\text{CC}}^N \times \text{Total Nitrogen Load} \times \text{Nitrogen Damage}}{\text{Mean MRBI Payments}} \quad (8)$$

where $\hat{\delta}_{\text{MRBI}}^{\text{CC}}$ is the 1.75 percentage-point increase in cover crop adoption attributed to MRBI (Section 4) and $\hat{\beta}_{\text{CC}}^N$ is the estimated 0.83% reduction in total nitrogen concentration with every one-percentage-point increase in upstream cover crop adoption share (Section 5). We compute the average total nitrogen load for targeted subwatersheds by combining total nitrogen concentrations with discharge rates at each monitoring station across the six states, as shown in Equation (9).

$$\text{Total Nitrogen Load}_{ym} = \sum_d (\text{Discharge Rate}_{ymd} \times \text{Total Nitrogen Concentration}_{ym}) \quad (9)$$

We monetize that reduction in nitrogen in surface water at \$16,100 per ton ([Sobota](#)

et al., 2015). As shown in the Table A4, this value is appropriate because it lies near the median of estimates in the literature on the social costs of nitrogen in the United States and encompasses multiple categories of damages. We acknowledge, however, that estimates in prior studies range widely, from a few hundred to several tens of thousands of dollars per ton, depending on the geographic scope, the share of applied nitrogen that enters the environment, the set of damage categories considered (e.g., impacts on fisheries, human health, or drinking water), and the valuation methods employed.

We compare the resulting monetary benefit to the average MRBI payments per targeted subwatershed to derive the BCR. Our back-of-the-envelope calculation yields an BCR of roughly 2.52 (95% confidence interval: [0.30, 4.73])¹⁰, reflecting only water pollution reduction benefits. This estimate likely represents a lower bound of the BCR for EQIP–MRBI, as it does not account for private benefits to farmers, such as improved cash crop yields and reduced production risk over the long term (Ma et al., 2023) and other social benefits such as soil carbon sequestration. This measure provides a useful baseline for assessing EQIP’s impact on nitrogen reduction and underscores how cover crops can help offset a portion of the broader damages caused by excess nitrogen.

7 Conclusions

This study evaluates the effectiveness of EQIP in promoting cover crop adoption and its subsequent impact on water quality in the Midwest. Using a novel 17-year satellite-derived dataset and harmonized water quality metrics, we find that EQIP–MRBI increased cover crop adoption share by 1.75 percentage points, with persistent effects beyond program funding, which is a 29% increase over baseline. At the same time, while EQIP subsidies generate persistent adoption of cover crop, their additionality is limited, underscoring the need for sharper targeting to enhance environmental effectiveness. Our empirical results suggest that a one percentage point increase in upstream cover crop adoption leads to a 0.83% reduction in total nitrogen concentration in surface water, while no statistically significant effect is observed for phosphorus. These findings highlight the potential of PES programs to mitigate nutrient pollution, while also underscoring challenges related to program design, targeting, and the adequacy of conservation subsidies. Although EQIP’s cover crop incentives recover 252% of their implementation costs through nitrogen pollution reduction, sustained impacts

¹⁰We calculate the 95% confidence interval of the BCR using the delta method assuming independence of $\hat{\delta}_{\text{MRBI}}^{\text{CC}}$ and $\hat{\beta}_{\text{CC}}^N$. If we assume a moderately positive correlation coefficient of 0.2 between $\hat{\delta}_{\text{MRBI}}^{\text{CC}}$ and $\hat{\beta}_{\text{CC}}^N$, reflecting that both parameters are likely influenced by common data and specification features, such as the same spatial or temporal shocks that tend to attenuate both effects in the same direction, creating a positive covariance, then we will get a wider confidence interval [0.09, 4.94].

will require greater and more consistent investment, particularly in effective regions where milder winter conditions enable cover crops to establish and generate substantial benefits. Enhancing long-term adoption and improving environmental targeting remain critical policy considerations, but these objectives cannot be achieved without adequate public funding.

Bibliography

- M. Abdalla, A. Hastings, K. Cheng, Q. Yue, D. Chadwick, M. Espenberg, J. Truu, R. M. Rees, and P. Smith. A critical review of the impacts of cover crops on nitrogen leaching, net greenhouse gas balance and crop productivity. *Global Change Biology*, 25(8):2530–2543, 2019. ISSN 1365-2486. doi: 10.1111/gcb.14644. URL <https://onlinelibrary.wiley.com/doi/abs/10.1111/gcb.14644>. eprint: <https://onlinelibrary.wiley.com/doi/pdf/10.1111/gcb.14644>.
- S. Aglasan, R. M. Rejesus, S. Hagen, and W. Salas. Cover crops, crop insurance losses, and resilience to extreme weather events. *American Journal of Agricultural Economics*, 106(4):1410–1434, 2024. ISSN 1467-8276. doi: 10.1111/ajae.12431. URL <https://onlinelibrary.wiley.com/doi/abs/10.1111/ajae.12431>. eprint: <https://onlinelibrary.wiley.com/doi/pdf/10.1111/ajae.12431>.
- M. P. Aillery. Contrasting Working-Land and Land Retirement Programs. Economic Brief 34093, United States Department of Agriculture, Economic Research Service, 2006. URL <https://ageconsearch.umn.edu/record/34093/files/eb060004.pdf>.
- K. M. Aspelund and A. Russo. Additionality and Asymmetric Information in Environmental Markets: Evidence from Conservation Auctions. 2023. URL <https://www.semanticscholar.org/paper/Additionality-and-Asymmetric-Information-in-from-Aspelund-Russo/2c2b51a93be9ceffcc752738d601a475d30cf749>.
- J. S. Bergtold, S. Ramsey, L. Maddy, and J. R. Williams. A review of economic considerations for cover crops as a conservation practice. *Renewable Agriculture and Food Systems*, 34(1):62–76, Feb. 2019. ISSN 17421705. doi: 10.1017/S1742170517000278. URL <https://www.proquest.com/docview/2253709211/abstract/AEBA5064FD841DCPQ/1>. Num Pages: 62-76 Place: Cambridge, United Kingdom Publisher: Cambridge University Press.
- H. Blanco-Canqui. Cover Crops and Water Quality. *Agronomy Journal*, 110(5):1633–1647, Sept. 2018. ISSN 0002-1962, 1435-0645. doi: 10.2134/agronj2018.02.0077. URL <https://onlinelibrary.wiley.com/doi/10.2134/agronj2018.02.0077>.
- L. Chen, R. M. Rejesus, S. Aglasan, S. C. Hagen, and W. Salas. The impact of cover crops on soil erosion in the US Midwest. *Journal of Environmental Management*, 324:116168, Dec. 2022. ISSN 0301-4797. doi: 10.1016/j.jenvman.2022.116168. URL <https://www.sciencedirect.com/science/article/pii/S0301479722017418>.
- R. Claassen, E. N. Duquette, and D. J. Smith. Additionality in U.S. Agricultural Conservation Programs. *Land Economics*, 94(1):19–35, Feb. 2018. ISSN 0023-7639, 1543-8325. doi: 10.3368/le.94.1.19. URL <https://le.uwpress.org/content/94/1/19>. Publisher: University of Wisconsin Press Section: Articles.
- J. R. Cober, M. L. Macrae, and L. L. Van Eerd. Nutrient Release from Living and Terminated Cover Crops Under Variable Freeze-Thaw Cycles. *Agronomy Journal*, 110(3):1036–1045, 2018. ISSN 1435-0645. doi: 10.2134/agronj2017.08.0449. URL <https://onlinelibrary.wiley.com/doi/abs/10.2134/agronj2017.08.0449>. eprint: <https://acsess.onlinelibrary.wiley.com/doi/pdf/10.2134/agronj2017.08.0449>.
- S. M. Dabney, J. A. Delgado, and D. W. Reeves. Using Winter Cover Crops to Improve Soil and Water Quality. *Communications in Soil Science and Plant Analysis*, 32(7-8):1221–1250, Apr. 2001. ISSN 0010-3624. doi: 10.1081/CSS-100104110. URL <https://doi.org/10.1081/CSS-100104110>. Publisher: Taylor & Francis eprint: <https://doi.org/10.1081/CSS-100104110>.

- C. de Chaisemartin and X. D'Haultfoeuille. Difference-in-Differences Estimators of Intertemporal Treatment Effects. *The Review of Economics and Statistics*, pages 1–45, Feb. 2024. ISSN 0034-6535. doi: 10.1162/rest_a_01414. URL https://doi.org/10.1162/rest_a_01414.
- W. K. Dodds, W. W. Bouska, J. L. Eitzmann, T. J. Pilger, K. L. Pitts, A. J. Riley, J. T. Schloesser, and D. J. Thornbrugh. Eutrophication of U.S. Freshwaters: Analysis of Potential Economic Damages. *Environmental Science & Technology*, 43(1):12–19, Jan. 2009. ISSN 0013-936X. doi: 10.1021/es801217q. URL <https://doi.org/10.1021/es801217q>. Publisher: American Chemical Society.
- N. K. Fageria, V. C. Baligar, and B. A. Bailey. Role of Cover Crops in Improving Soil and Row Crop Productivity. *Communications in Soil Science and Plant Analysis*, 36(19-20):2733–2757, Oct. 2005. ISSN 0010-3624. doi: 10.1080/00103620500303939. URL <https://doi.org/10.1080/00103620500303939>. Publisher: Taylor & Francis .eprint: <https://doi.org/10.1080/00103620500303939>.
- H. Feng, L. A. Kurkalova, C. L. Kling, and P. W. Gassman. Environmental conservation in agriculture: Land retirement vs. changing practices on working land. *Journal of Environmental Economics and Management*, 52(2):600–614, Sept. 2006. ISSN 0095-0696. doi: 10.1016/j.jeem.2006.03.004. URL <https://www.sciencedirect.com/science/article/pii/S0095069606000453>.
- P. Fleming. Agricultural Cost Sharing and Water Quality in the Chesapeake Bay: Estimating Indirect Effects of Environmental Payments. *American Journal of Agricultural Economics*, 99(5):1208–1227, 2017. ISSN 1467-8276. doi: 10.1093/ajae/aax040. URL <https://onlinelibrary.wiley.com/doi/abs/10.1093/ajae/aax040>. .eprint: <https://onlinelibrary.wiley.com/doi/pdf/10.1093/ajae/aax040>.
- P. Fleming, E. Lichtenberg, and D. A. Newburn. Evaluating impacts of agricultural cost sharing on water quality: Additionality, crowding In, and slippage. *Journal of Environmental Economics and Management*, 92:1–19, Nov. 2018. ISSN 0095-0696. doi: 10.1016/j.jeem.2018.08.007. URL <https://www.sciencedirect.com/science/article/pii/S0095069617303467>.
- GAO. Agricultural Conservation: USDA's Environmental Quality Incentives Program Could Be Improved to Optimize Benefits | U.S. GAO. Technical report, U.S. Government Accountability Office, Apr. 2017. URL <https://www.gao.gov/products/gao-17-225>.
- B. R. Hanrahan, K. W. King, E. W. Duncan, and V. S. Shedekar. Cover crops differentially influenced nitrogen and phosphorus loss in tile drainage and surface runoff from agricultural fields in Ohio, USA. *Journal of Environmental Management*, 293:112910, Sept. 2021. ISSN 0301-4797. doi: 10.1016/j.jenvman.2021.112910. URL <https://www.sciencedirect.com/science/article/pii/S0301479721009725>.
- H.-C. Hsieh and B. M. Gramig. Estimating the impact of cover crop adoption on ambient nitrogen concentration in the upper Mississippi River drainage. *Applied Economic Perspectives and Policy*, 46(2):609–626, 2024. ISSN 2040-5804. doi: 10.1002/aepp.13408. URL <https://onlinelibrary.wiley.com/doi/abs/10.1002/aepp.13408>. .eprint: <https://onlinelibrary.wiley.com/doi/pdf/10.1002/aepp.13408>.
- B. K. Jack. Private Information and the Allocation of Land Use Subsidies in Malawi. *American Economic Journal: Applied Economics*, 5(3):113–135, July 2013. ISSN 1945-7782. doi: 10.1257/app.5.3.113. URL <https://www.aeaweb.org/articles?id=10.1257/app.5.3.113>.
- B. K. Jack and S. Jayachandran. Self-selection into payments for ecosystem services pro-

- grams. *Proceedings of the National Academy of Sciences*, 116(12):5326–5333, Mar. 2019. doi: 10.1073/pnas.1802868115. URL <https://www.pnas.org/doi/abs/10.1073/pnas.1802868115>. Publisher: Proceedings of the National Academy of Sciences.
- N. Karwowski and M. Skidmore. Nature's Kidneys: the Role of the Wetland Reserve Program in Restoring Water Quality. 2023.
- J. P. Kaye and M. Quemada. Using cover crops to mitigate and adapt to climate change. A review. *Agronomy for Sustainable Development*, 37(1):4, Jan. 2017. ISSN 1773-0155. doi: 10.1007/s13593-016-0410-x. URL <https://doi.org/10.1007/s13593-016-0410-x>.
- D. A. Keiser, C. L. Kling, and J. S. Shapiro. The low but uncertain measured benefits of US water quality policy. *Proceedings of the National Academy of Sciences*, 116(12):5262–5269, Mar. 2019. ISSN 0027-8424, 1091-6490. doi: 10.1073/pnas.1802870115. URL <https://pnas.org/doi/full/10.1073/pnas.1802870115>.
- A. P. Kinzig, C. Perrings, F. S. Chapin, S. Polasky, V. K. Smith, D. Tilman, and B. L. Turner. Paying for Ecosystem Services—Promise and Peril. *Science*, 334(6056):603–604, Nov. 2011. doi: 10.1126/science.1210297. URL <https://www.science.org/doi/full/10.1126/science.1210297>. Publisher: American Association for the Advancement of Science.
- E. Krasovich, P. Lau, J. Tseng, J. Longmate, K. Bell, and S. Hsiang. Harmonized nitrogen and phosphorus concentrations in the Mississippi/Atchafalaya River Basin from 1980 to 2018. *Scientific Data*, 9(1):524, Aug. 2022. ISSN 2052-4463. doi: 10.1038/s41597-022-01650-6. URL <https://www.nature.com/articles/s41597-022-01650-6>. Publisher: Nature Publishing Group.
- R. Kudela, E. Berdalet, and E. Urban. Harmful Algal Blooms : A scientific summary for policy makers. June 2015. doi: 10.13039/100005243. URL <https://digital.csic.es/handle/10261/141712>. Accepted: 2016-12-20T12:43:37Z Publisher: Unesco.
- K. Larson. Additionality and Duration in Cover Cropping Incentives, 2024. Published: Available upon request.
- K. H. Lee, T. M. Isenhart, and R. C. Schultz. Sediment and nutrient removal in an established multi-species riparian buffer. *Journal of Soil and Water Conservation*, 58(1):1–8, Jan. 2003. ISSN 0022-4561, 1941-3300. URL <https://www.jswconline.org/content/58/1/1>. Publisher: Soil and Water Conservation Society Section: Research Section.
- P. Liu, Y. Wang, and W. Zhang. The influence of the Environmental Quality Incentives Program on local water quality. *American Journal of Agricultural Economics*, 105(1):27–51, Jan. 2023. ISSN 0002-9092, 1467-8276. doi: 10.1111/ajae.12316. URL <https://onlinelibrary.wiley.com/doi/10.1111/ajae.12316>.
- M. Ma, C. Reeling, M. N. Hughes, S. Armstrong, and R. Roth. Comparison of conservation instruments under long-run yield uncertainty and farmer risk aversion. *European Review of Agricultural Economics*, 50(5):1685–1714, Dec. 2023. ISSN 0165-1587. doi: 10.1093/erae/jbad029. URL <https://doi.org/10.1093/erae/jbad029>.
- K. Metaxoglou and A. Smith. Agriculture's nitrogen legacy. *Journal of Environmental Economics and Management*, 130:103132, Mar. 2025. ISSN 0095-0696. doi: 10.1016/j.jeem.2025.103132. URL <https://www.sciencedirect.com/science/article/pii/S0095069625000166>.
- S. Pathak, H. Wang, D. Q. Tran, and N. C. Adusumilli. Persistence and disadop-

- tion of sustainable agricultural practices in the Mississippi Delta region. *Agronomy Journal*, 116(2):765–776, 2024. ISSN 1435-0645. doi: 10.1002/agj2.21519. URL <https://onlinelibrary.wiley.com/doi/abs/10.1002/agj2.21519>. _eprint: <https://acsess.onlinelibrary.wiley.com/doi/pdf/10.1002/agj2.21519>.
- A. Plastina, W. Sawadgo, and E. Okonkwo. Pervasive Disadoption Substantially Offsets New Adoption of Cover Crops and No-Till. *Choices: The Magazine of Food, Farm, and Resource Issues*, 39(02), 2024. doi: 10.22004/ag.econ.344738. URL <https://EconPapers.repec.org/RePEc:ags:aaeach:344738>. Publisher: Agricultural and Applied Economics Association.
- G. E. Roesch-McNally, A. D. Basche, J. Arbuckle, J. C. Tyndall, F. E. Miguez, T. Bowman, and R. Clay. The trouble with cover crops: Farmers' experiences with overcoming barriers to adoption. *Renewable Agriculture and Food Systems*, 33(4):322–333, Aug. 2018. ISSN 1742-1705, 1742-1713. doi: 10.1017/S1742170517000096. URL https://www.cambridge.org/core/product/identifier/S1742170517000096/type/journal_article.
- A. B. Rosenberg, B. Pratt, and D. Szmurlo. Impacts of an increase in federal assistance for cover cropping: Evidence from the Environmental Quality Incentives Program. *American Journal of Agricultural Economics*, 107(3):795–825, 2025. ISSN 1467-8276. doi: 10.1111/ajae.12502. URL <https://onlinelibrary.wiley.com/doi/abs/10.1111/ajae.12502>. _eprint: <https://onlinelibrary.wiley.com/doi/pdf/10.1111/ajae.12502>.
- J. Salzman, G. Bennett, N. Carroll, A. Goldstein, and M. Jenkins. The global status and trends of Payments for Ecosystem Services. *Nature Sustainability*, 1(3):136–144, Mar. 2018. ISSN 2398-9629. doi: 10.1038/s41893-018-0033-0. URL <https://www.nature.com/articles/s41893-018-0033-0>. Number: 3 Publisher: Nature Publishing Group.
- M. Sarrantonio and E. Gallandt. The Role of Cover Crops in North American Cropping Systems. *Journal of Crop Production*, 8(1-2):53–74, Feb. 2003. ISSN 1092-678X. doi: 10.1300/J144v08n01_04. URL https://doi.org/10.1300/J144v08n01_04. Publisher: Taylor & Francis _eprint: https://doi.org/10.1300/J144v08n01_04.
- W. Sawadgo and A. Plastina. Do cost-share programs increase cover crop use? Empirical evidence from Iowa. *Renewable Agriculture and Food Systems*, 36(6):527–535, Dec. 2021. ISSN 1742-1705, 1742-1713. doi: 10.1017/S1742170521000132. URL <https://www.cambridge.org/core/journals/renewable-agriculture-and-food-systems/article/do-costshare-programs-increase-cover-crop-use-empirical-evidence-from-iowa/83B2FCF05B192C5BFFB374B115E9A55A>.
- W. P. M. Sawadgo, W. Zhang, and A. Plastina. What drives landowners' conservation decisions? Evidence from Iowa. *Journal of Soil and Water Conservation*, 76(3):211–221, May 2021. ISSN 0022-4561, 1941-3300. doi: 10.2489/jswc.2021.00115. URL <https://www.jswconline.org/content/76/3/211>. Publisher: Soil and Water Conservation Society Section: Research Section.
- W. Schlenker and M. J. Roberts. Nonlinear temperature effects indicate severe damages to U.S. crop yields under climate change. *Proceedings of the National Academy of Sciences*, 106(37): 15594–15598, Sept. 2009. doi: 10.1073/pnas.0906865106. URL <https://www.pnas.org/doi/abs/10.1073/pnas.0906865106>. Publisher: Proceedings of the National Academy of Sciences.
- C. A. Seifert, G. Azzari, and D. B. Lobell. Satellite detection of cover crops and their effects on crop yield in the Midwestern United States. *Environmental Research Letters*, 13(6):064033, June

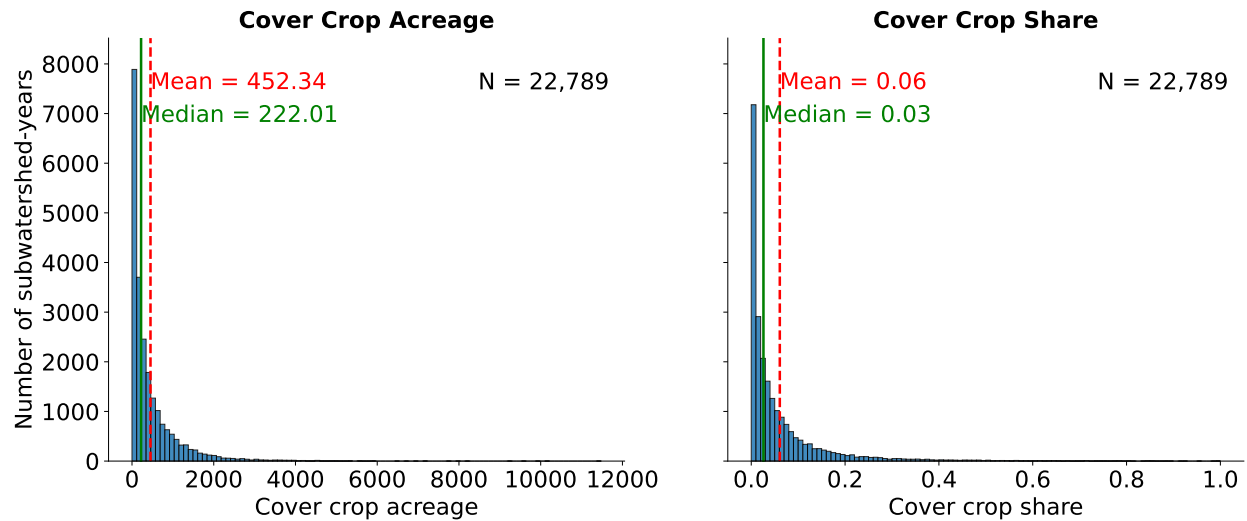
2018. ISSN 1748-9326. doi: 10.1088/1748-9326/aac4c8. URL <https://dx.doi.org/10.1088/1748-9326/aac4c8>. Publisher: IOP Publishing.
- A. N. Sharpley and S. Smith. Effects of cover crops on surface water quality. *Cover crops for clean water*, pages 41–49, 1991. Publisher: Soil and Water Conservation Society Ankeny, IA.
- D. J. Sobota, J. E. Compton, M. L. McCrackin, and S. Singh. Cost of reactive nitrogen release from human activities to the environment in the United States. *Environmental Research Letters*, 10(2):025006, Feb. 2015. ISSN 1748-9326. doi: 10.1088/1748-9326/10/2/025006. URL <https://dx.doi.org/10.1088/1748-9326/10/2/025006>. Publisher: IOP Publishing.
- C. Tonitto, M. B. David, and L. E. Drinkwater. Replacing bare fallows with cover crops in fertilizer-intensive cropping systems: A meta-analysis of crop yield and N dynamics. *Agriculture, Ecosystems & Environment*, 112(1):58–72, Jan. 2006. ISSN 0167-8809. doi: 10.1016/j.agee.2005.07.003. URL <https://www.sciencedirect.com/science/article/pii/S0167880905003749>.
- USDA NRCS. Conservation Practices on Cultivated Cropland: A Comparison of CEAP I and CEAP II Survey Data and Modeling. Technical report, U.S. Department of Agriculture, Natural Resources Conservation Service, Washington, D.C., Mar. 2022. URL <https://www.nrcs.usda.gov/ceap>.
- USDA OIG. Environmental Quality Incentives Program (EQIP). Technical Report Audit Report 10601-0001-31, U.S. Department of Agriculture, Office of Inspector General, July 2014.
- M. H. Ward, R. R. Jones, J. D. Brender, T. M. de Kok, P. J. Weyer, B. T. Nolan, C. M. Villanueva, and S. G. van Breda. Drinking Water Nitrate and Human Health: An Updated Review. *International Journal of Environmental Research and Public Health*, 15(7):1557, July 2018. ISSN 1661-7827. doi: 10.3390/ijerph15071557. URL <https://www.ncbi.nlm.nih.gov/pmc/articles/PMC6068531/>.
- S. Won, R. M. Rejesus, B. K. Goodwin, and S. Aglasan. Understanding the effect of cover crop use on prevented planting losses. *American Journal of Agricultural Economics*, 106(2):659–683, 2024. ISSN 1467-8276. doi: 10.1111/ajae.12396. URL <https://onlinelibrary.wiley.com/doi/abs/10.1111/ajae.12396>. eprint: <https://onlinelibrary.wiley.com/doi/pdf/10.1111/ajae.12396>.
- T. Zhang, R. Iovanna, and C. Kling. The Effects of Conservation Reserve Program On Downstream Water Quality Across the US, May 2025. URL <https://papers.ssrn.com/abstract=5247549>.

Appendices

A Supplemental Figures and Tables	41
B Institutional Appendix: EQIP and MRBI	48
B.1 The EQIP Mechanism	48
B.2 The MRBI Mechanism	49
B.3 Hydrologic Unit Hierarchy	50
C Background on Nutrient Pollution and Cover Crops	51
C.1 Nutrient Pollution	51
C.2 How Cover Crops Reduce Nutrient Pollution	52
C.3 Private Incentives for Cover Crop Adoption	52
D Data Appendix	54
D.1 Cover Crop Adoption Data	54
D.2 Weather	61
D.3 Soil Characteristics	62
E Robustness and Heterogeneity Analyses	63
E.1 Heterogeneity by State	63
Appendix References	66

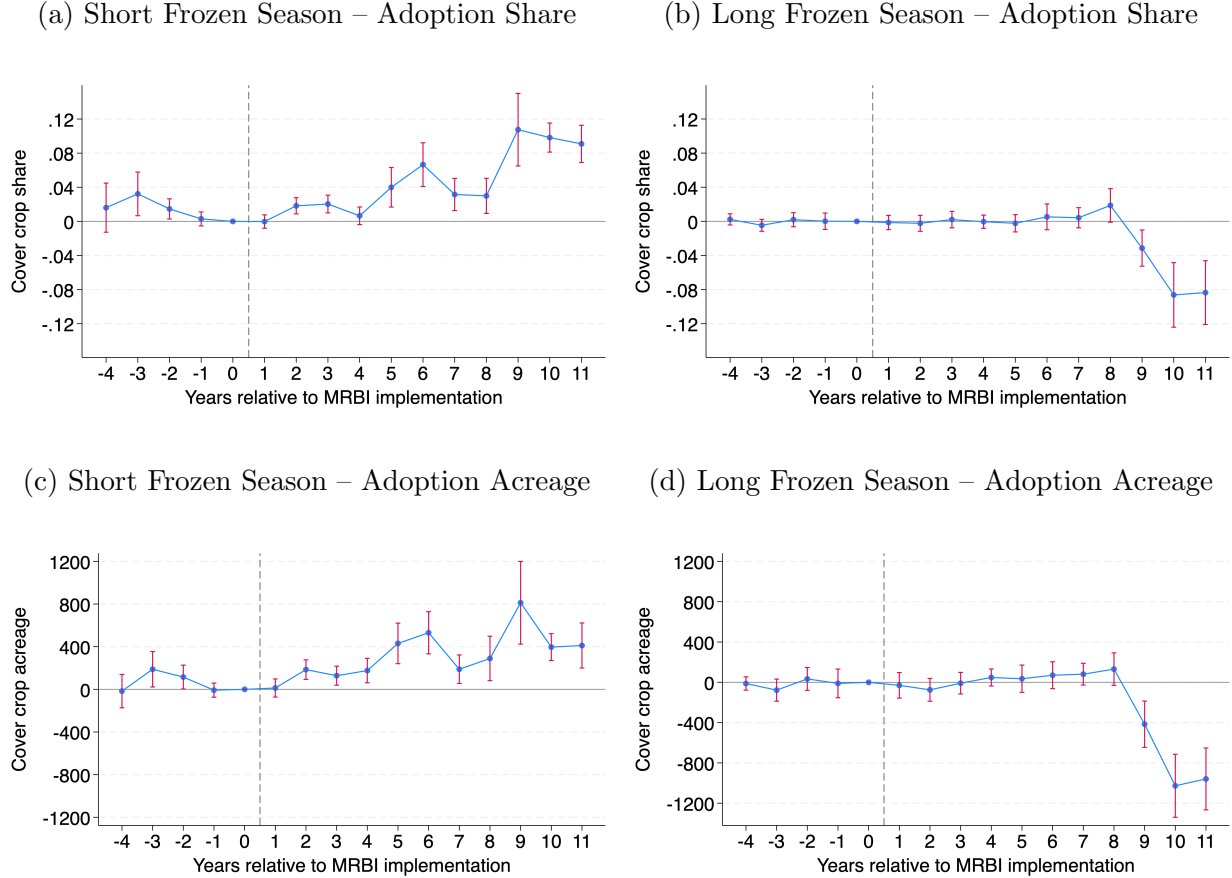
A Supplemental Figures and Tables

Figure A1: Distribution of Cover Crop Acreage and Share across Subwatershed–Years



Note: This figure shows histograms of cover crop acreage (left) and cover crop share (right) across subwatershed–years. The y-axis represents the count of subwatershed–years by bin. Vertical lines mark the mean (red, dashed) and median (green, solid) values for each distribution. Data cover the period 2008–2023 and include all subwatersheds in MRBI priority areas after excluding those ever treated under NWQI and those not intersecting with states where treated subwatersheds are located.

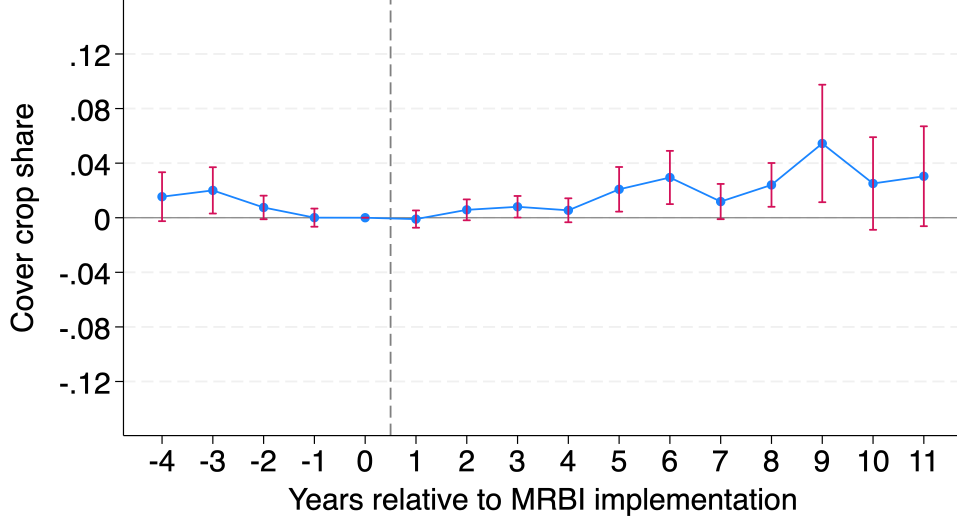
Figure A2: Event-Study Estimates of EQIP–MRBI Effects on Cover Crop Adoption: Short vs. Long Frozen Seasons



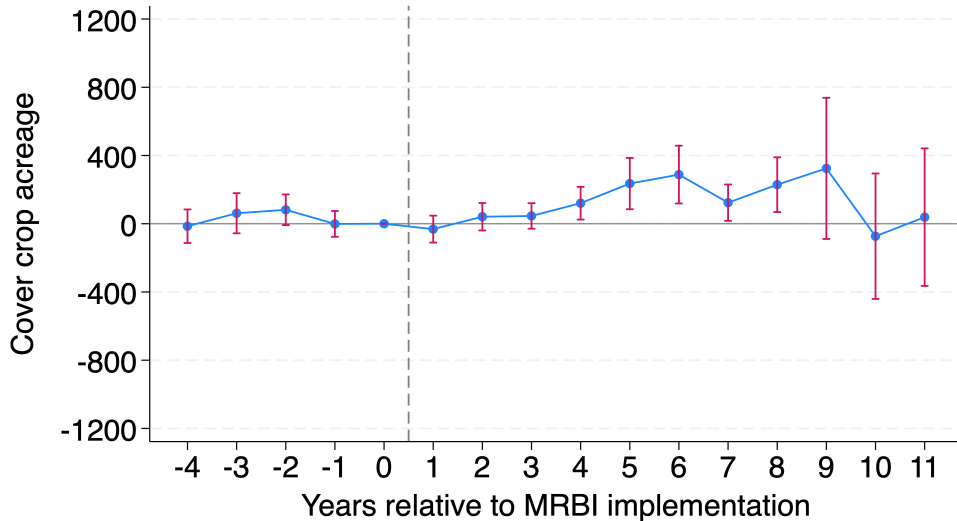
Note: The figure presents estimates from a difference-in-differences event-study design in Equation (3) following [de Chaisemartin and D'Haultfoeuille \(2024\)](#). The top panels present results using cover crop adoption share as the outcome, while the bottom panels present results using adoption acreage, separately for subwatersheds with shorter frozen seasons (average length: 65 days) and longer frozen seasons (average length: 112 days). Frozen season length is defined as the number of days between the first date with at least three consecutive days of mean temperature below 0°C, based on 30-year climate normals from 1991 to 2020. All coefficients are estimates relative to the baseline year immediately preceding project implementation ($t=0$). The horizontal line at 0 marks this baseline, and the vertical dashed grey line corresponds to the year of MRBI initiative implementation. Standard errors are clustered at the HUC-12 level. Red bars indicate 95% confidence intervals.

Figure A3: Effects of MRBI on Cover Crop Adoption with Matching DID

(a) Cover Crop Share

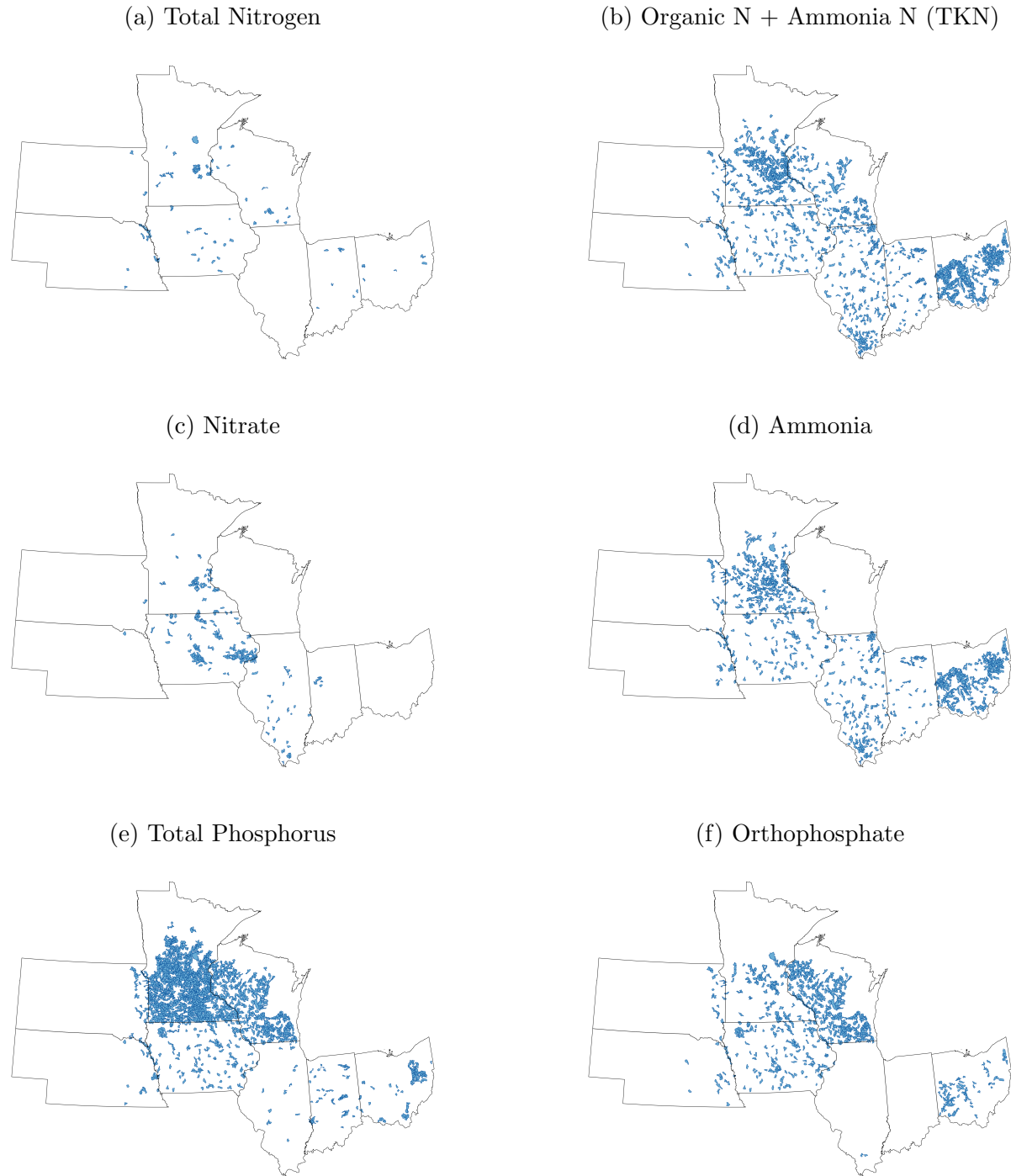


(b) Cover Crop Acreage



Note: The figure presents estimates from a difference-in-differences event-study design in Equation (3) [de Chaisemartin and D'Haultfœuille \(2024\)](#), estimated on a matched comparison set with matching weights. Matching covariates: pre-treatment cover crop-share trend, three-year average cropped acreage, soil productivity indices, slope, and soil water properties. Panel (a) reports results using cover crop adoption acreage as the outcome, while panel (b) uses the adoption share. All coefficients are estimates relative to the baseline year immediately preceding project implementation ($t=0$). The horizontal line at 0 marks this baseline, and the vertical dashed grey line corresponds to the year of MRBI initiative implementation. Standard errors are clustered at the HUC-12 level. Red bars indicate 95% confidence intervals. The analysis uses an unbalanced panel of HUC-12 watersheds from 2008–2023, consisting of 209 ever-treated HUC-12s and 1,262 never-treated controls, for a total of 16,803 HUC12–year observations and 1,064 treatment switch periods.

Figure A4: Subwatersheds with Multiple Monitoring Stations by Compound Type



Note: The figure maps subwatersheds with multiple water-quality monitoring stations used in the regressions following Equation (6), categorized by compound type. Blue shading highlights subwatersheds that contain two or more monitoring stations operating for more than 30 months and recording the corresponding compound type. Because the regressions include subwatershed-by-year fixed effects, all identification comes from subwatersheds with at least two monitoring stations, which provide within-subwatershed-year variation in upstream and downstream cover crop adoption share measurements. Each panel corresponds to a specific compound—total nitrogen (TN), total Kjeldahl nitrogen (TKN), nitrate, ammonia, total phosphorus (total phosphorus), and orthophosphate—with spatial patterns reflecting differences in monitoring coverage and data duration across compounds.

Table A1: Comparison of Estimated Effects of Cover Crops on Nitrogen Outcomes Across Studies

Study	Context	Methods	Effect Size
Hsieh and Gramig (2024)	Midwest, 2008–2018, across-subbasin variation	Panel FE	↑ 1 pp CC ⇒ ↓ 2% TN
Liu et al. (2023)	U.S., 2005–2015, across-watershed variation	Upstream-downstream DID	↑ 10% EQIP payments ⇒ ↓ 0.29% TN
Hanrahan et al. (2021)	Northcentral Ohio, 2012-2019, field experiments	Edge-of-field monitor, Wilcoxon Test	↓ 52% TN in tile drainage, ↓ 6% TN in surface runoff
This paper	Midwest, 2007-2018, within-subwatershed variation	Panel FE controlling cover crop downstream	↑ 1 pp CC ⇒ ↓ 0.88% total nitrogen (TN)

Table A2: Comparison of Estimated Effects of Cover Crops on Phosphorus Outcomes Across Studies

Study	Context	Methods	Effect Size
Liu et al. (2023)	U.S., 2005–2015, across-watershed variation	Upstream-downstream DID	↑ 10% EQIP payments ⇒ ↑ 0.23% TP
Hanrahan et al. (2021)	Northcentral Ohio, 2012-2019, field experiments	Edge-of-field monitor, Wilcoxon Test	↑ 7% dissolved reactive phosphorous (DRP) in tile drainage, ↓ 16% DRP in surface runoff
This paper	Midwest, 2007-2018, within-subwatershed variation	Panel FE controlling cover crop downstream	No effect on TP, ↑ 1 pp CC ⇒ ↑ 0.53% orthophosphate

Table A3: Robustness Checks Using Daily Data and Expanded Fixed Effects

	(1)	(2)	(3)	(4)	(5)	(6)
Panel A. No Controls						
Cover Crop Upstream	-1.433*** (0.140)	-0.975*** (0.172)	-0.369*** (0.113)	-0.719** (0.343)	-1.432*** (0.265)	-0.300** (0.130)
Panel B. Controls						
Cover Crop Upstream	-1.093*** (0.127)	-0.807*** (0.200)	-0.351*** (0.109)	-0.813** (0.343)	-0.927*** (0.246)	-0.314** (0.125)
Panel C. Controls + Placebo						
Cover Crop Upstream	-0.523*** (0.169)	-0.799*** (0.268)	-0.241* (0.137)	-0.842** (0.355)	-0.572* (0.334)	-0.216 (0.137)
Panel D. Controls + ≥50 obs						
Cover Crop Upstream	-0.925*** (0.133)	-1.115*** (0.158)	-0.474*** (0.169)	-0.654* (0.368)	-1.238*** (0.206)	-0.470** (0.190)
Fixed Effects	year × month + DOY	hue8 + year × month + DOY	hue12 + year × month + DOY	hue12 × year + year × month + DOY	state × year + year × month + DOY	MLI + year × month + DOY

Notes: The table reports robustness check results using daily water quality data instead of monthly averages and including additional fixed effects such as year-by-month interactions and day-of-year (DOY) controls. Columns vary by the set of fixed effects, while rows vary by the inclusion of control variables, placebo variables, and the minimum number of observations per site. Across all specifications, the effect of upstream cover crop adoption share remains negative and statistically significant, with effect sizes comparable to those from the main specification, supporting the robustness of the main findings.

Table A4: Economic damages from nitrogen pollution across different studies

Source	Damages	Geographic Scope
Taylor and Heal (2021)	\$583	U.S., per ton of nitrogen applied
Sobota et al. (2015)	\$16,100	U.S., per ton of nitrogen
Van Grinsven et al. (2013)	\$13,338–\$53,351	E.U., per ton of nitrogen
Compton et al. (2011)	\$56,000	GoM fisheries decline, per ton of nitrogen
Compton et al. (2011)	\$6,380	CB recreational use, per ton of nitrogen
Von Blottnitz et al. (2006)	\$300	E.U., per ton of nitrogen
Dodds et al. (2009)	\$2.2 billion	U.S., freshwater eutrophication, annually
Kudela et al. (2015)	\$4.6 billion	U.S., algal blooms, annually
Boehm et al. (2020)	\$0.552–\$2.4 billion	GoM fisheries & marine habitat, annually
Anderson et al. (2000)	\$449 million	U.S., algal blooms, annually

Notes: This table is adapted from [Metaxoglou and Smith \(2025\)](#). This table summarizes estimates of damages caused by nitrogen pollution from various studies. Damages are presented in monetary terms per ton of nitrogen or as annual aggregate damages, depending on the study. The geographic scope indicates the region for which the damage estimates apply. Estimates vary depending on scope and valuation methods. Abbreviations: U.S. = United States, E.U. = European Union, GoM = Gulf of Mexico, CB = Chesapeake Bay.

B Institutional Appendix: EQIP and MRBI

B.1 The EQIP Mechanism

EQIP, administered by the USDA NRCS, provides financial and technical assistance to farmers, ranchers, and nonindustrial private forest landowners to plan and implement conservation practices that improve soil health, water quality, and other environmental outcomes on agricultural land.

The Food Security Act of 1985, as amended by subsequent farm bills in 2002, 2008, 2014, and 2018, specifies that EQIP's purpose includes optimizing environmental benefits. However, its cost-effectiveness has been a point of controversy. Reports from the Office of Inspector General (OIG) have found that NRCS's methods for allocating EQIP funds to states and distribution within states have not sufficiently prioritized environmental concerns. Furthermore, while EQIP is designed to enhance environmental outcomes, the NRCS ranking tool used to assess applications does not accurately measure environmental benefits, and cost-effectiveness is given only a 10% weight—insufficient to meaningfully impact the selection process ([USDA OIG, 2014](#); [GAO, 2017](#)).

To fulfill this goal, the USDA NRCS develops national conservation priorities and determines each state office's funding allocation, including nationally targeted initiatives and discretionary amounts for state offices. The state offices then address state-specific environmental issues and distribute EQIP funds.

The program follows a structured process: Producers submit applications to local NRCS offices voluntarily, which are then evaluated and ranked within funding pools based on environmental benefit and cost-effectiveness. Selected applicants enter into contracts specifying the approved practices and implementation schedules. Once practices are completed and verified to meet NRCS standards, participants receive cost-share payments, which typically cover a portion of installation costs.

The program reimbursed producers a percentage (up to 75 percent) of actual costs from the implementation of conservation practices from 1996 to 2008 and conducts payments based on a payment schedule depending on state-determined cost estimates starting in 2009. Nowadays, payments are generally made at flat rates that vary by conservation practice, state, and specific program guidelines. Payment schedules are determined at the state level, based on standardized practice scenarios developed at the regional level by the NRCS. Each state establishes cost-share rates for approved practices, generally covering up to 75 percent of the estimated implementation cost for most producers.

Historically underserved farmers, including beginning, socially disadvantaged, limited-

resource, and veteran producers, are eligible for higher cost-share rates of up to 90 percent and may also receive advance payments to help cover up-front expenses prior to implementation. EQIP contracts may range from one to ten years, although most are shorter. In the case of cover crop practices, contract periods generally last no more than five years.



B.2 The MRBI Mechanism

The MRBI was launched in 2009 as a targeted conservation effort under EQIP to reduce nutrient runoff and improve water quality across the Mississippi River Basin. MRBI operates in twelve participating states, including Illinois, Indiana, Iowa, Minnesota, Ohio, and Wisconsin. Within the Basin, the NRCS designates subbasin-level priority zones based on nutrient-loading and water-quality impairments. Each state retains discretion in selecting specific subwatersheds and implementation partners—such as state agencies, conservation districts, and nonprofit organizations—to carry out watershed projects.

Each MRBI project generally includes a readiness (planning) phase of up to two years followed by a three- to five-year implementation phase. During implementation, producers enroll in EQIP and sign multi-year contracts to adopt approved conservation practices (e.g., cover crops, nutrient management, residue management). EQIP contracts obligated under MRBI are subject to the same terms and conditions as other EQIP contracts. Although project funding for new enrollments is limited to the implementation period, EQIP contracts signed under MRBI may extend beyond the project’s official end date, as participants remain obligated to maintain practices for the full contract term, which typically is up to five years.

Although NRCS issues national guidance, state NRCS offices determine their own partner-selection and watershed-ranking criteria, tailoring the process to local priorities and capacity.

For example, Minnesota’s State Technical Committee applies a point-based watershed-selection system as below.

- **Documentation of Pollution Issues and Planning** (0–40 points): evaluates the presence of water-quality plans and analyses, including Total Maximum Daily Load (TMDL) reports, Watershed Restoration and Protection Strategies (WRAPS), Groundwater Restoration and Protection Strategies (GRAPS), hydrologic-function analyses, and comprehensive watershed plans such as One Watershed, One Plan. Watersheds receive higher scores when these documents explicitly link identified pollutant sources to proposed interventions and include measurable monitoring frameworks.

- **Local Readiness** (0–40 points): measures the strength of partnerships, leadership capacity, producer willingness, and outreach. Points are awarded for clearly defined lead organizations, formal partnership agreements or letters of support, farmer commitments, co-funding, and detailed outreach and community-engagement plans.
- **Multiple Benefits** (0–20 points): credits projects that deliver co-benefits beyond water-quality improvement (e.g., wildlife or pollinator habitat, flood-reduction, soil-health, or air-quality benefits—and) that align with complementary state or regional plans (e.g., Minnesota Prairie Conservation Plan or Drinking-Water Supply Management Plans).

These point-based criteria serve as an example of how MRBI projects are prioritized at the state level. While the specific indicators and weights differ across states, most apply comparable principles.

MRBI therefore integrates EQIP’s practice-based contracting framework with state-specific spatial targeting and competitive selection, enabling NRCS to focus limited conservation funds in watersheds where conservation practices are expected to yield the highest environmental returns.

B.3 Hydrologic Unit Hierarchy

Hydrologic units are standardized geographic areas delineated by the U.S. Geological Survey (USGS) based on surface water drainage patterns. Each unit is assigned a unique Hydrologic Unit Code (HUC) that follows a hierarchical structure: larger regions are divided into progressively smaller units, including subregions (HUC-4), basins (HUC-6), subbasins (HUC-8), watersheds (HUC-10), and subwatersheds (HUC-12). A subbasin (HUC-8) represents a medium-scale drainage area, while a subwatershed (HUC-12) represents a smaller tributary area nested within a subbasin. Figure 2 illustrates the spatial extent of subbasins (red boundaries) and subwatersheds (blue filled units) used in the analysis.

C Background on Nutrient Pollution and Cover Crops

C.1 Nutrient Pollution

Nitrogen and phosphorus, essential nutrients for all life forms, are fundamental components of commercial fertilizers. Excessive fertilizer usually occurs in high-performing yield regions (with high values of the percentage of the observed to attainable yield), including the U.S. These excessive nutrients can easily run off into surface water or leach into groundwater during heavy rainfall, leading to serious environmental and economic issues.

Eutrophication, a major consequence of nutrient overabundance in water bodies, leads to rapid algae and aquatic plant growth, disrupting ecosystems and recreational activities. This process depletes oxygen and blocks sunlight, essential for underwater life, eventually creating uninhabitable "dead zones." The Gulf of Mexico hosts the U.S.'s largest dead zone, spanning about 6,500 square miles each summer, primarily due to nutrient runoff from the Mississippi River Basin. Additionally, harmful algae blooms can produce toxins, posing severe risks to wildlife, pets, and humans. Recent estimates suggest that nitrogen and phosphorus pollution costs the U.S. at least \$4.6 billion annually, with the greatest losses attributed to diminished property values and recreational uses of water ([Kudela et al., 2015](#)). Implementing regenerative agricultural practices upstream could offer a cost-effective solution by enhancing soil quality and productivity benefits to the farmers themselves and providing a positive externality to the downstream water bodies.

Moreover, nitrogen pollution presents serious health hazards, particularly in areas reliant on private water sources in heavily farmed regions, which suffer from inadequate monitoring and regulation. The U.S. has set the maximum contaminant level for nitrate in drinking water at 10 mg/L as nitrate-nitrogen (NO₃-N) to prevent infant methemoglobinemia, or "blue baby syndrome." However, this does not account for other health effects. Long-term exposure to nitrate levels below the standard may still pose health risks, including colorectal cancer, thyroid disease, and neural tube defects, as nitrates are converted into carcinogenic compounds within the digestive system ([Ward et al., 2018](#)). Articles indicate a concerning level of nitrate contamination across U.S. water systems. For instance, Iowa has documented more than 7,000 private water wells contaminated with nitrates, and more than 200 of Iowa's community water systems struggle with high nitrate levels, periodically issuing "Do Not Drink" orders (Keith Schneider, 2023).

C.2 How Cover Crops Reduce Nutrient Pollution

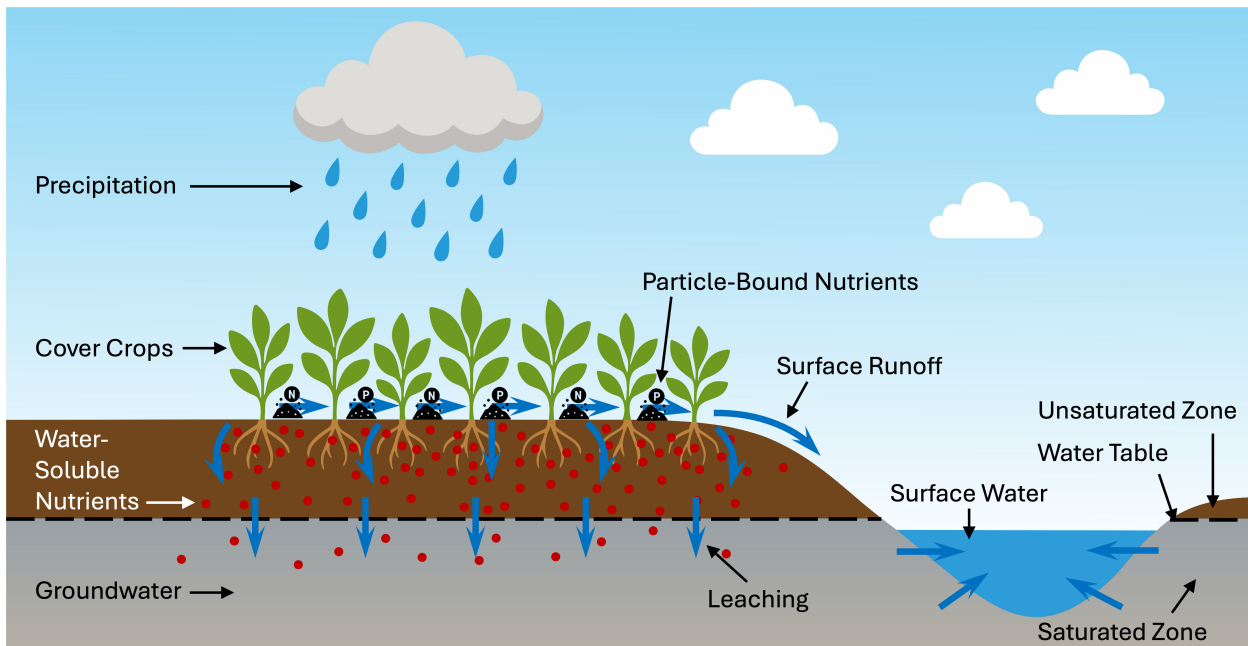
Nutrients from agricultural fields reach surface waters through two main hydrological pathways: surface runoff and subsurface leaching (see Figure A5). Surface runoff transports particle-bound nitrogen and phosphorus compounds during rainfall events. At the same time, subsurface leaching moves dissolved nutrients such as nitrate and dissolved phosphorus (mainly orthophosphate) through groundwater and tile drainage systems, which eventually discharge into streams and rivers. In the Midwest, the water table is relatively high and artificial drainage is widespread, making subsurface leaching an essential contributor to nutrient loading in surface waters alongside runoff.

Cover crops mitigate nutrient losses through both channels. In the short run, their vegetation provides a physical barrier that reduces runoff and erosion and actively takes up residual soil nitrogen, thereby lowering leaching (Blanco-Canqui, 2018; Abdalla et al., 2019). However, decomposition of plant residues before the next cash crop can temporarily release nutrients, increasing the potential for leaching. As a result, empirical studies report mixed effects of cover crops on water quality, particularly for soluble nutrients (Hanrahan et al., 2021; Cober et al., 2018; Sharpley and Smith, 1991). In the long run, cover crops enhance soil organic carbon, structure, and water-holding capacity, which further reduces nutrient losses through both runoff and leaching (Blanco-Canqui, 2018; Abdalla et al., 2019).

C.3 Private Incentives for Cover Crop Adoption

From an economic perspective, farmers adopt cover crops only when the expected private benefits exceed the costs of establishment, management, and potential yield penalties on subsequent cash crops. In the short term, these costs often outweigh the private gains from improved soil fertility or risk reduction (Bergtold et al., 2019; Roesch-McNally et al., 2018). It may also be linked to the primary cash crop yield losses during the initial years of cover crop adoption (Ma et al., 2023). There are also concerns that heavy plant residues from cover crops might increase susceptibility to pests and weeds (Aiyer et al., 2024; Extension, 2021). The benefits of enhanced soil organic carbon, nutrient retention, and water-holding capacity accumulate slowly, making them difficult to capture within a single lease or planning horizon. Institutional factors further dampen adoption. Tenant farmers—who operate a large share of Midwestern cropland—lack long-term incentives to invest in soil health improvements on rented land (Sawadgo et al., 2021). Timing of spring termination and equipment requirements adds to perceived risk. Consequently, cost-share and technical-assistance programs such as EQIP and MRBI play a crucial role in overcoming these short-term disincentives and aligning private decisions with socially optimal conservation outcomes.

Figure A5: Pathways of Nutrient Loss and the Role of Cover Crops in Mitigation



Note: This figure illustrates how nutrients from agricultural fields reach surface water through two primary hydrological pathways: surface runoff and subsurface leaching. Particle-bound nitrogen (N) and phosphorus (P) compounds are transported via runoff during rainfall events, while nitrate leaching occurs through groundwater or tile drainage systems, ultimately contributing to baseflow pollution. Cover crops reduce nutrient losses by decreasing runoff and erosion, and by taking up residual nutrients in the soil. However, residue decomposition before the next planting season can temporarily increase soluble nutrient leaching. Over time, cover crops improve soil structure, organic carbon content, and water-holding capacity, mitigating both runoff- and leaching-related nutrient losses.

D Data Appendix

D.1 Cover Crop Adoption Data

The algorithm outlined in Figure A6 below presents our sophisticated approach for detecting and analyzing winter cover crops by integrating remote sensing data, USDA survey data, climate data, and machine learning techniques.

D.1.1 Satellite Data Processing and Vegetation Index Construction

In this paper, we develop a Python pipeline that leverages Google Earth Engine (GEE) to automatically retrieve Landsat 5, 7, and 8 imagery from 2007 to 2024, compute vegetation indices, and aggregate pixel-level information to field-level boundaries.

First, to ensure consistency and reduce contamination from atmospheric interference, we apply a quality assurance mask using the *QA_PIXEL* band to exclude pixels affected by clouds, cloud shadows, and snow or ice.

Second, we calculate 18 vegetation indices (see Table A5) for each pixel, including soil-adjusted ones that perform well in areas with low biomass on the ground. We display the indices and their formula in Table 1 below. These indices are constructed using atmospherically corrected surface reflectance products from the USGS Landsat Level 2, Collection 2, Tier 1 Dataset.

Third, we extract the mean values of each vegetation index at the field level by spatially reducing the imagery over field boundaries derived from the Common Land Unit (CLU) dataset. We use the 2007 CLU dataset to define field boundaries, under the assumption that parcel boundaries remain relatively stable over time. More recent versions of the CLU dataset are no longer publicly available due to privacy restrictions. To minimize edge effects and reduce noise in vegetation signals near field borders, we apply a 30-meter inward buffer to each field. For each Landsat image, we compute field-level average values and annotate them with the image acquisition date.

Fourth, to manage computational load and memory limits in GEE, the dataset is processed in chunks of 1,000 fields at a time, with spatial clipping using convex hulls buffered around each subset.

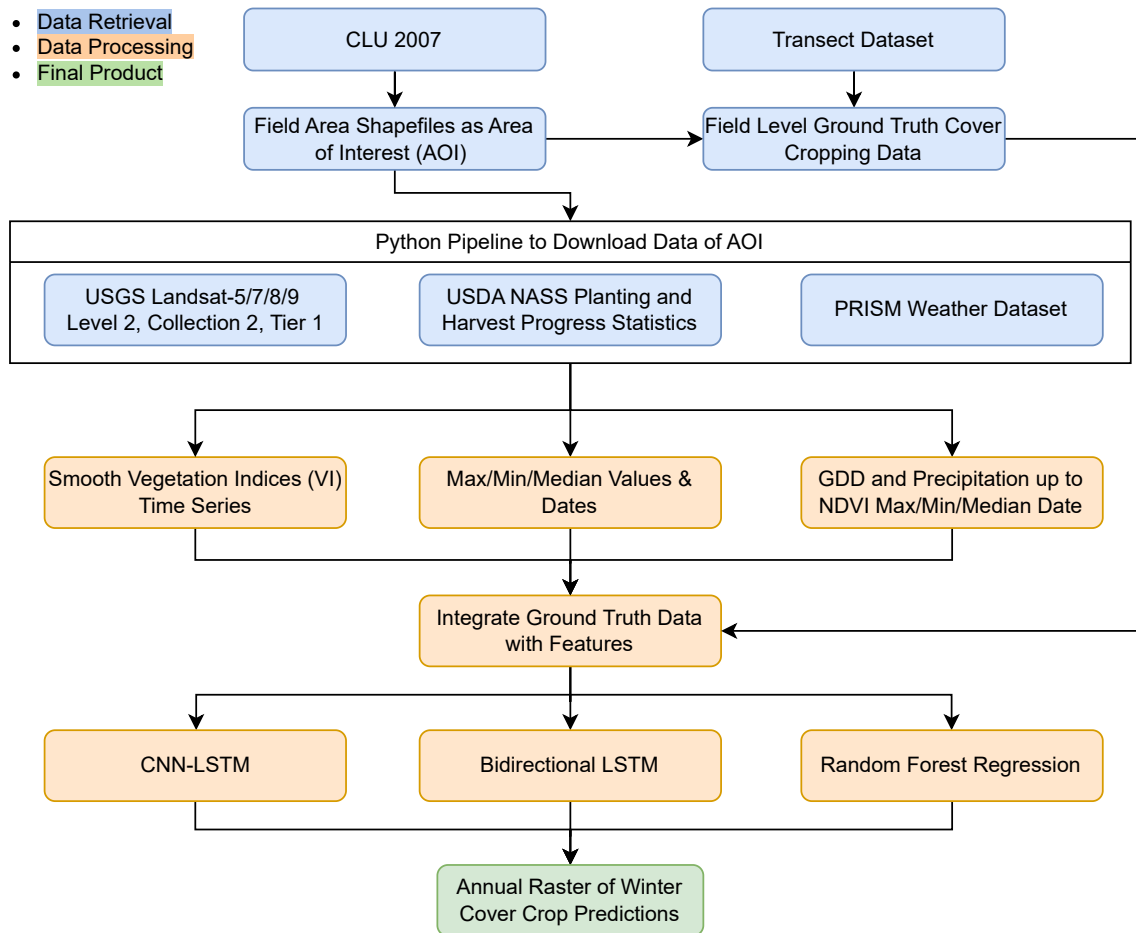
The final dataset comprises field-level, date-stamped observations of all raw bands available through the Landsat dataset, as well as multiple vegetation indices constructed. They are exported in CSV format for downstream analysis.

Table A5: Vegetation Indices Derived from Landsat-7 Surface Reflectance

Index	Definition	Definition based on Landsat-7 Details	Reference
NDVI	$\frac{\rho_{\text{NIR}} - \rho_{\text{Red}}}{\rho_{\text{NIR}} + \rho_{\text{Red}}}$	$\frac{B4 - B3}{B4 + B3}$	Rouse et al. (1974)
TVI	$\left(\frac{\rho_{\text{NIR}} - \rho_{\text{Red}}}{\rho_{\text{NIR}} + \rho_{\text{Red}}} + 0.5 \right)^{1/2} \times 100$	$\left(\frac{B4 - B3}{B4 + B3} + 0.5 \right)^{1/2} \times 100$	Nellis and Briggs (1992)
EVI	$G \frac{\rho_{\text{NIR}} - \rho_{\text{Red}}}{\rho_{\text{NIR}} + C_1 \rho_{\text{Red}} - C_2 \rho_{\text{Blue}} + L}$	$G \frac{B4 - B3}{B4 + C_1 B3 - C_2 B1 + L}$	Huet et al. (2002)
SATVI	$\frac{\rho_{\text{SWIR1}} - \rho_{\text{Red}}}{\rho_{\text{SWIR1}} + \rho_{\text{Red}} + L} (1 + L) - \frac{\rho_{\text{SWIR2}}}{2}$	$\frac{B5 - B3}{B5 + B3 + L} (1 + L) - \frac{B7}{2}$	Soil Adjusted Total VI (arid/semiarid soils); $L = 1$ commonly. Marssett et al. (2006)
SAVI	$\frac{(\rho_{\text{NIR}} - \rho_{\text{Red}})(1+L)}{\rho_{\text{NIR}} + \rho_{\text{Red}} + L}$	$\frac{(B4 - B3)(1+L)}{B4 + B3 + L}$	Soil-adjusted VI; $L = 0.5$ typical. Huete (1988)
MSI	$\frac{\rho_{\text{SWIR1}}}{\rho_{\text{NIR}}}$	$\frac{B5}{B4}$	Moisture Stress Index (higher = drier). ROCK (1985)
GNDVI	$\frac{\rho_{\text{NIR}} - \rho_{\text{Green}}}{\rho_{\text{NIR}} + \rho_{\text{Green}}}$	$\frac{B4 - B2}{B4 + B2}$	Green NDVI (chlorophyll sensitivity). Gitelson et al. (1996)
GRVI	$\frac{\rho_{\text{NIR}} - \rho_{\text{Red}}}{\rho_{\text{Green}} - \rho_{\text{Red}}}$	$\frac{B2 - B3}{B2 + B3}$	Green–Red Vegetation Index. Tucker (1979)
LSWI	$\frac{\rho_{\text{NIR}} - \rho_{\text{SWIR1}}}{\rho_{\text{NIR}} + \rho_{\text{SWIR1}}}$	$\frac{B4 - B5}{B4 + B5}$	Land Surface Water Index (canopy/water moisture). Xiao et al. (2004)
55 TSAVI	$\frac{s(B4 - sB3 - a)}{aB4 + B3 - as + X(1+s^2)}$	Transformed SAVI using soil-line parameters (a, s) and adjustment X .	Baret and Guyot (1991)
MSAVI	$\frac{(1+L)(\rho_{\text{NIR}} - \rho_{\text{Red}})}{\rho_{\text{NIR}} + \rho_{\text{Red}} + L}$	$\frac{(1+L)(B4 - B3)}{B4 + B3 - L}$	Modified SAVI; reduces soil background effects. Qi et al. (1994a)
MSAVI2	$\frac{2\rho_{\text{NIR}} + 1 - \sqrt{(2\rho_{\text{NIR}} + 1)^2 - 8(\rho_{\text{NIR}} - \rho_{\text{Red}})}}{2}$	$\frac{2B4 + 1 - \sqrt{(2B4 + 1)^2 - 8(B4 - B3)}}{2}$	Closed-form MSAVII; no L parameter required. Qi et al. (1994b)
WDVI	$\rho_{\text{NIR}} - C \rho_{\text{Red}}$	$B4 - C B3$	Weighted Difference Vegetation Index; C is the slope of the Red–NIR soil line estimated from bare-soil pixels (not a per-pixel ratio). Clevers (1988)
BI	$\frac{\sqrt{(\rho_{\text{Red}})^2 + (\rho_{\text{Green}})^2}}{2}$	$\frac{\sqrt{(B3)^2 + (B2)^2}}{2}$	Brightness Index (two-band version). Escadafal (1989)
BI2	$\sqrt{\frac{(\rho_{\text{Red}})^2 + (\rho_{\text{Green}})^2 + (\rho_{\text{NIR}})^2}{3}}$	$\frac{\sqrt{(B3)^2 + (B2)^2 + (B4)^2}}{3}$	Brightness Index (three-band version). Escadafal (1989)
RI	$\frac{(\rho_{\text{Red}})^2}{(\rho_{\text{Green}})^2}$	$\frac{(B3)^2}{(B2)^2}$	Red/Green Ratio Index; sensitive to soil reflectance. Pouget et al. (1991)
CI	$\frac{\rho_{\text{Red}} - \rho_{\text{Green}}}{\rho_{\text{Red}} + \rho_{\text{Green}}}$	$\frac{B3 - B2}{B3 + B2}$	Color Index; higher for bare soil and senescent vegetation. Pouget et al. (1991)
V	$\frac{\rho_{\text{NIR}}}{\rho_{\text{Red}}}$	$\frac{B4}{B3}$	Simple vegetation ratio (Jordan's VI). Jordan (1969)

Notes: This table lists the 18 vegetation indices calculated for each pixel using atmospherically corrected surface reflectance from the USGS Landsat 7 Level 2, Collection 2, Tier 1 dataset. Definitions are provided in both generic form and in terms of Landsat 7 spectral bands. The indices include normalized difference, soil-adjusted, and moisture-related metrics commonly used to characterize vegetation vigor, canopy cover, and soil background effects.

Figure A6: Algorithm for Identifying Cover Crops Using Remote Sensing Data



Note: This figure presents the algorithm diagram used to generate annual field-level cover crop predictions across the U.S. Midwest. The process begins with field area shapefiles that define the area of interest (AOI). A Python-based pipeline retrieves satellite imagery from USGS Landsat 5, 7, and 8 Level-2 Collection 2 Tier-1 datasets, alongside USDA NASS planting and harvest progress data, PRISM weather variables, and 2007 CLU boundaries. Ground-truth field-level cover crop data are integrated with smoothed vegetation index (VI) time series and derived features such as growing degree days (GDD) and precipitation up to the NDVI maximum, minimum, and median dates. Machine-learning models, including Random Forest, Convolutional Neural Network–Long Short-Term Memory (CNN–LSTM), and Bidirectional LSTM, are trained to predict winter cover crop presence for each pixel. The final product is an annual raster map of winter cover crop adoption aggregated at the field level.

D.1.2 Data Harmonization and Interpolation

We harmonize and clean the field-level Landsat 5, 7, and 8 datasets to ensure consistency across sensors, eliminate cloud-covered observations, and obtain more frequent observations. Combining Landsat 5, 7, and 8 imagery from Collection 2 Level-2 Tier 1 is standard practice, as USGS's Collection 2 processing streamlines radiometry, geometry, and *QA* across sensors so that data from different missions are considered analysis-ready without additional harmonization. We standardize the column names since band naming conventions differ slightly between sensors. For each field and date, duplicate observations are resolved by retaining the one with the lowest atmospheric opacity, measured by the *SR_ATMOS_OPACITY* value, as a proxy for image quality. Additionally, we filter out invalid records based on reflectance thresholds (e.g., $SR_B2 \geq 50,000$), which may indicate sensor artifacts or residual cloud contamination.

To produce temporally regular and noise-reduced time series for each field, we implement a temporal alignment and interpolation procedure for all available variables. First, we snap all observation dates to the nearest 7-day interval to align data across fields with different imaging schedules. Second, we apply a custom function to smooth the time series if there are large sharp dips in vegetation indices, indicating the presence of undetected clouds or shadows. Finally, we use the Piecewise Cubic Hermite Interpolating Polynomial (PCHIP) method to interpolate the data, fill in the missing values, and thus construct a complete time series with 7-day intervals. PCHIP provides a smooth approximation while preserving the monotonicity and shape of the original data, as we assume that biomass generally changes gradually and that high-frequency noise in vegetation indices often stems from radiometric variability rather than true ecological signals.

The final output is a harmonized, field-level vegetation index dataset suitable for downstream analysis. It includes field-level time series data at 7-day intervals spanning 2007 to 2024, with each observation containing both the original and interpolated values for all bands from the satellite and 12 vegetation indices. The dataset is well-suited for modeling biomass dynamics and detecting management practices such as cover cropping.

D.1.3 Determination of Fall and Spring Cover Crop Growing Seasons

This study determines the annual critical freezing dates based on the PRISM daily average temperature dataset and thereby decides the fall and spring growth windows of cover crops. The core of the algorithm lies in identifying the first non-freezing day of each spring (i.e., the earliest continuous warm period after the last freezing event in the spring) and the end of the non-freezing period in each fall (i.e., the latest warm period before the first freezing

event in fall or winter). The specific process is as follows:

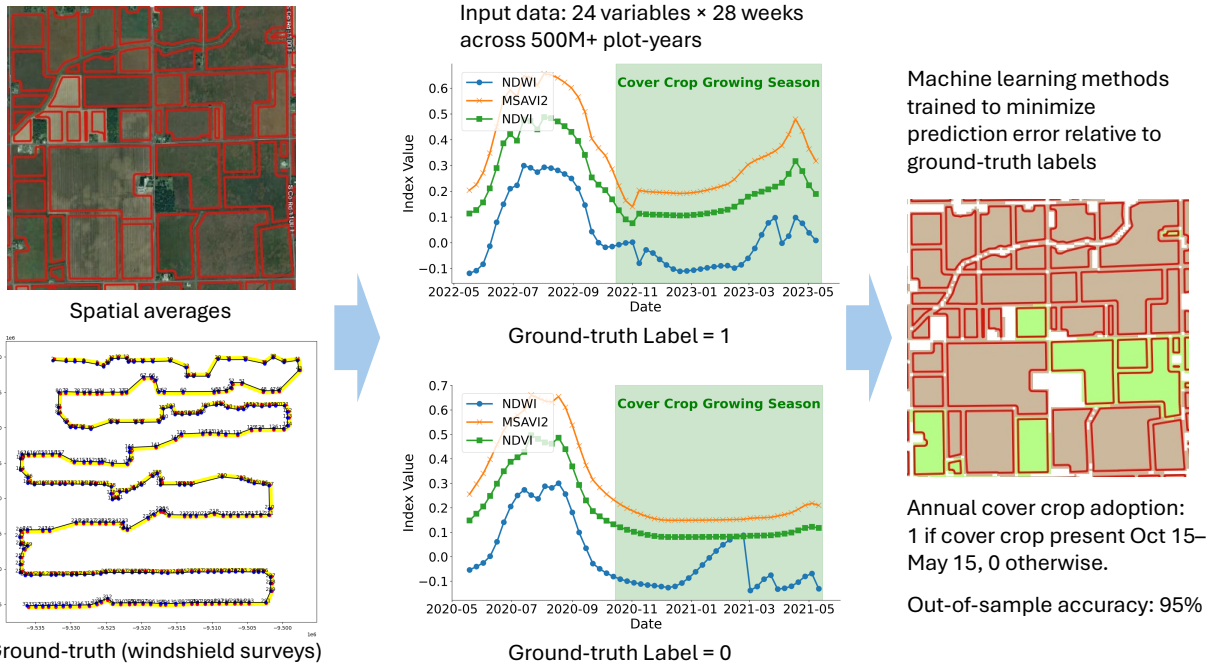
First, we utilize the Google Earth Engine API to retrieve county-level administrative boundaries for Midwestern states and extract the spatial average of daily mean temperature data from the PRISM dataset for the period 2007–2024. For each county and year, we construct a daily temperature series spanning January 1 to December 31. Second, we identify consecutive 3-day periods with average temperatures above 0 °C (i.e., freeze-free conditions) with a moving window approach. Third, we record the earliest such period in a given year as the spring reference date, marking the start of the safe planting window, and the latest such period as the fall reference date, indicating the end of the freeze-free season. The three-day criterion filters out short-term fluctuations and enables a more robust and conservative identification of sustained non-freezing intervals.

We then define the growth window period of cover crops based on the definition of non-freezing days and the harvest and planting season of the cash crops. We define the fall cover crop season as the period from the median harvest date of the cash crop to one week after the last frost-free day in the fall or winter. The spring cover crop season is defined as the period from one week before the first frost-free day in the spring to two weeks before the median planting date. Cover crops typically require 4 to 8 weeks before the fall reference date or 6 to 10 weeks after the spring reference date to germinate and accumulate sufficient biomass (Nagila et al., 2022; SARE, 2021). Additionally, we also take into account the harvest and planting times of cash crops. The region we study lies within the zone where cover crops are typically terminated at or before cash crop planting, and in some areas, even before crop emergence (USDA NRCS, 2019). Accordingly, we define the end of the spring cover crop growing season as the median planting date of corn or soybeans. We extract state-and year-specific median planting and harvesting dates from USDA NASS Crop Progress and Condition survey data. We extend the fall and spring seasons by one week beyond the last and before the first non-freezing dates, respectively, to better capture the whole growth cycle of cover crops and reduce false negatives in detection. This buffer helps ensure that we do not miss vegetation signals indicative of cover cropping. This adjustment is critical given the imbalance in the ground truth data, where non-cover-cropped fields substantially outnumber cover-cropped ones. Accurate identification of cover-cropped fields is therefore essential for improving model performance.

D.1.4 Model Training and Performance

We began by partitioning the dataset into two parts: a training and validation set comprising 90% of the observations, and an untouched test set comprising the remaining 10%. The test set was held out at the start and used only once at the end to evaluate the final ensemble,

Figure A7: Workflow for Constructing the field-Level Cover Crop Dataset



Note: This figure illustrates the workflow used to construct the annual field-level cover crop dataset across the U.S. Midwest. Satellite imagery from Landsat 5, 7, and 8 was processed into 24 time-varying spectral and vegetation variables for each pixel, which were then averaged within each field and interpolated into 24 weekly time series spanning 28 weeks per year, covering more than 500 million field-year observations. Ground-truth labels were obtained from windshield surveys that recorded whether cover crops were present in fall and spring during each observation year. Machine-learning models were trained to minimize prediction error relative to these labels, achieving an out-of-sample accuracy of approximately 95.1%. Annual cover crop adoption is defined as 1 if a cover crop was detected between October 15 and May 15 and 0 otherwise.

ensuring an unbiased estimate of generalization.

Within the training and validation split, we applied a five-fold cross-validation procedure. In each fold, four subsets were used for training and one for validation, rotating across folds so that every observation contributed once to validation. To prepare the data for modeling, we standardized features using a StandardScaler fitted only on the training partition, applying the transformation consistently across validation and test observations.

On each fold we trained two deep learning architectures, a convolutional neural network with a long short-term memory layer (CNN-LSTM) and a bidirectional long short-term memory network (BiLSTM), and a random forest model. Sequence inputs into the deep learning models were organized as length-28 time series with 24 features, preserving the temporal structure of the original signals. And the data input to the random forest model include 140 features for each plot-year. The CNN-LSTM consisted of a one-dimensional convolution over the time dimension, followed by a two-layer LSTM with hidden size 128, with the last hidden state passed through a fully connected layer to produce a binary logit. The BiLSTM employed a two-layer bidirectional LSTM of the same hidden size, followed by a nonlinear dense layer with dropout and a final output node. Both models were trained with the Adam optimizer using a learning rate of 0.0005 and weight decay of 1e-5. The loss function was binary cross-entropy with logits, augmented by a positive-class weight equal to the ratio of negative to positive examples in each training fold in order to address class imbalance. Training was conducted for up to forty epochs, and the best model from each fold was selected on the basis of validation performance measured by the area under the precision-recall curve (PR-AUC). We also trained a random forest regressor with 1,000 trees and a maximum depth of 40. Class imbalance was addressed by applying class weights so that minority outcomes were upweighted relative to majority outcomes during training. Random forests operate by fitting each decision tree to a bootstrap sample of the data while randomly subsampling features at each split, thereby reducing correlation across trees and improving generalization. The final prediction is obtained by aggregating the outputs of all trees, which allows the model to capture nonlinearities and complex interactions among predictors without requiring strong parametric assumptions.

The three models are incorporated into an ensemble framework. The motivation for ensembling is that different model classes capture different structures in the data: the deep learning models are designed to extract temporal dynamics from sequential covariates, whereas the random forest performs well on tabular predictors and can model nonlinear threshold effects more directly. By stacking the predictions from each model with a meta-learner, we leverage the complementary strengths of these approaches, reduce the risk of overfitting to any single model, and achieve more stable and accurate predictions on the

held-out test set.

To combine information across models, we implemented a stacking procedure. Out-of-fold predictions from the CNN-LSTM, BiLSTM, and random forest models on the validation partitions were collected and used as inputs to a logistic regression meta-learner. This meta-learner was then applied to the untouched test set by first generating predictions from both base models and passing them through the trained logistic regression. The resulting ensemble predictions were averaged across folds to provide the final classification output. Model performance was assessed using average precision as the primary metric, with additional reporting of ROC-AUC, F1 score, accuracy, balanced accuracy, and Cohen’s kappa. To summarize classification performance, thresholds were swept on the validation predictions to identify the value that maximized the F1 score, and this threshold was used as a reference when reporting results.

The final stacked model demonstrates strong predictive performance on the held-out test set. Averaged across the five cross-validation folds, the ensemble achieves 95.07% overall accuracy, indicating that the majority of field-year observations are correctly classified. However, given the imbalance between positive and negative outcomes in the data, accuracy alone is not sufficient to assess model quality. The F1 score of 0.73 reflects a balanced trade-off between precision and recall, showing that the model is effective at identifying cover crop adoption while limiting false positives. The PR-AUC reaches 0.80, further underscoring the model’s robustness in distinguishing positive cases in an imbalanced setting. Finally, Cohen’s kappa of 0.71 confirms substantial agreement between predicted and observed outcomes beyond chance. Taken together, these metrics indicate that the CNN-LSTM, BiLSTM, and random forest ensemble, combined through stacking, provides a reliable tool for predicting cover crop adoption at the field level.

D.2 Weather

The PRISM dataset integrates observations from multiple monitoring networks, uses spatial interpolation techniques, and provides realized weather information at approximately 4-kilometer resolution. The CDL offers 30-meter resolution land cover classifications annually distinguishing cultivated cropland from other land uses based on satellite imagery and decision-tree classification methods.

To isolate agricultural areas, we generate annual crop masks by identifying pixels classified as “cultivated” in the CDL each year. These masks are applied to the daily temperature and precipitation rasters, retaining values for agricultural pixels and excluding those for other types of pixels. We compute extreme degree days (EDDs), a widely used measurement in the

literature that captures heat stress relevant to agricultural production ([Schlenker et al., 2006](#); [Schlenker and Roberts, 2009](#); [Ortiz-Bobea, 2020](#)). We define EDD measures as cumulative exposure to harmful temperatures above a crop-specific threshold:

$$EDD = \frac{1}{T} \sum_{t=1}^T \max(Temp_t - TempBase, 0)$$

where T is the number of days in the growing season, $Temp_t$ is the maximum temperature on day t , and $TempBase$ is the temperature threshold to define the extreme temperature, which could be different for each crop. Following [Ortiz-Bobea \(2020\)](#), we set the threshold at 30 °C, a value commonly used to assess the impact of extreme heat on maize yields in the U.S.

We compute EDDs at the pixel level based on the masked temperature data and aggregate the pixel-level EDDs to the county level, averaging spatially within each county boundary. This procedure is repeated across all days in the growing season and for each year, producing a panel of county-by-year extreme weather variables.

D.3 Soil Characteristics

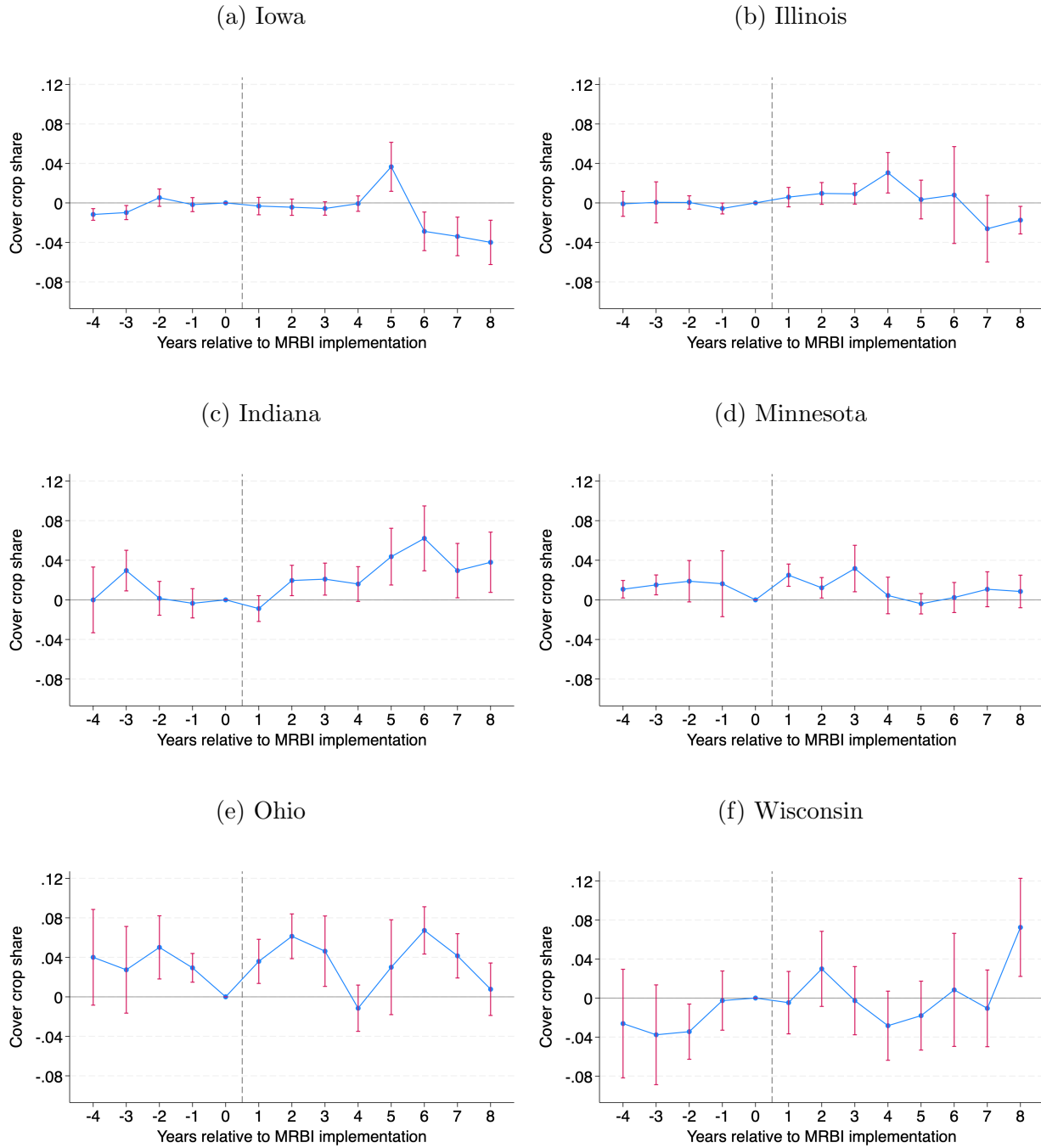
We use the gridded National Soil Survey Geographic Database (gNATSGO), a 30 m raster dataset that harmonizes SSURGO, STATSGO2, and the National Soil Information System into a seamless, high-resolution soil property surface. The dataset includes a rich set of variables relevant to soil quality, agronomy, and environmental outcomes. Specifically, we extract available water storage (AWS, mm) at multiple depth ranges (e.g., 0–5 cm, 0–20 cm, 0–100 cm, and intermediate layers such as 20–50 cm or 50–100 cm); soil organic carbon stocks (SOC, g C/m²) over analogous depth intervals; and derived metrics such as rooting zone available water, root zone effective rooting depth (emc), and droughtiness indices. We also incorporate categorical crop productivity ratings (NCCPI v3), including overall index and crop-specific values for corn and soybeans. For each farm plot CLU polygon, we compute spatial means of continuous attributes, yielding field-level soil indicators that capture heterogeneity in water holding capacity, organic matter content, rooting conditions, and crop productivity potential.

E Robustness and Heterogeneity Analyses

E.1 Heterogeneity by State

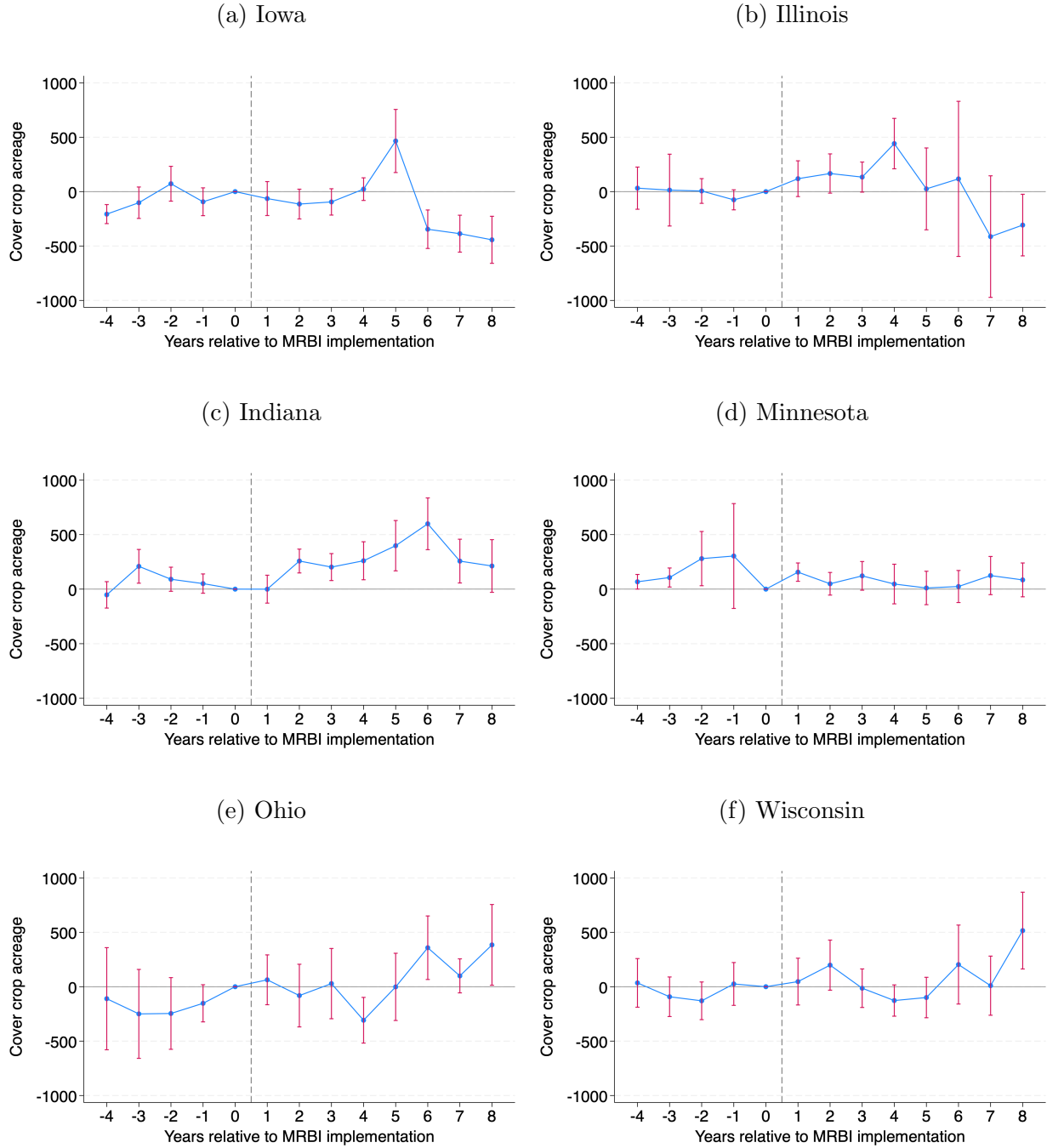
This section explores how the effects of EQIP–MRBI on cover crop adoption vary across states. Because each state has discretion in project design, outreach, and technical assistance, implementation may differ substantially. However, the number of treated subwatersheds within some states (e.g., Wisconsin) is relatively small, which limits statistical power. Consequently, these state-level estimates should be viewed as descriptive patterns rather than causal effects. The corresponding event-study results are shown in Figures A8 and A9. The results show substantial differences across states. Indiana’s strong and most persistent response might reflect higher program penetration, stronger outreach, or more favorable agronomic conditions. Iowa and Illinois experience moderate gains that build in the middle years but appear to taper off or even have negative effects in later years. Farmers in these states may have tried the program for a short period and then decide to drop out. This is consistent with evidence from the literature that the yield effects of cover crops do not show up until 5 to 8 years of continuous adoption (Ma et al., 2023). Ohio exhibits noisy and uncertain effects, with a statistically significant pre-trend, suggesting that they might be targeting high-adoption areas. The positive impacts observed after implementation could largely reflect a return to pre-existing trends, with sporadic years showing no effects, potentially affected by unobserved shocks. Both Minnesota and Wisconsin show only minor effects on cover crop adoption, which return to pre-treatment levels once the treatment ends, suggesting the program had limited impacts in these states.

Figure A8: Event Study of MRBI Effects on Cover Crop Share, by State



Note: The figure presents estimates from a difference-in-differences event-study design in Equation (3) following [de Chaisemartin and D'Haultfœuille \(2024\)](#). Each panel reports results using cover crop adoption acreage as the outcome, separately by state. All coefficients are estimates relative to the baseline year immediately preceding project implementation ($t=0$). The horizontal line at 0 marks this baseline, and the vertical dashed grey line corresponds to the year of MRBI initiative implementation. Standard errors are clustered at the HUC-12 level. Red bars indicate 95% confidence intervals.

Figure A9: Event Study of MRBI Effects on Cover Crop Acreage, by State



Note: The figure presents estimates from a difference-in-differences event-study design in Equation (3) following [de Chaisemartin and D'Haultfœuille \(2024\)](#). Each panel reports results using cover crop adoption acreage as the outcome, separately by state. All coefficients are estimates relative to the baseline year immediately preceding project implementation ($t=0$). The horizontal line at 0 marks this baseline, and the vertical dashed grey line corresponds to the year of MRBI initiative implementation. Standard errors are clustered at the HUC-12 level. Red bars indicate 95% confidence intervals.

Appendix References

- Harini S. Aiyer, Andrew McKenzie-Gopsill, Aaron Mills, and Adam John Foster. Select Cover Crop Residue and Soil Microbiomes Contribute to Suppression of Fusarium Root and Crown Rot in Barley and Soybean. *Microorganisms*, 12(2):404, February 2024. ISSN 2076-2607. doi: 10.3390/microorganisms12020404. URL <https://pmc.ncbi.nlm.nih.gov/articles/PMC10891762/>.
- Donald M. Anderson, Porter Hoagland, Yoshi Kaoru, and Alan W. White. Estimated Annual Economic Impacts from Harmful Algal Blooms (HABs) in the United States. Technical Report WHOI-2000-11, Woods Hole Oceanographic Institution, Woods Hole, MA, 2000. URL <https://www.whoi.edu/>.
- F. Baret and G. Guyot. Potentials and limits of vegetation indices for LAI and APAR assessment. *Remote Sensing of Environment*, 35(2):161–173, February 1991. ISSN 0034-4257. doi: 10.1016/0034-4257(91)90009-U. URL <https://www.sciencedirect.com/science/article/pii/003442579190009U>.
- Jason S. Bergtold, Steven Ramsey, Lucas Maddy, and Jeffery R. Williams. A review of economic considerations for cover crops as a conservation practice. *Renewable Agriculture and Food Systems*, 34(1):62–76, February 2019. ISSN 17421705. doi: 10.1017/S1742170517000278. URL <https://www.proquest.com/docview/2253709211/abstract/AEBA5064FD841DCPQ/1>. Num Pages: 62-76 Place: Cambridge, United Kingdom Publisher: Cambridge University Press.
- Rebecca Boehm, Don Anair, and Amine Mahmassani. Reviving the Dead Zone: Solutions to Benefit Both Gulf Coast Fishers and Midwest Farmers. Technical report, Union of Concerned Scientists, Cambridge, MA, June 2020. URL <http://www.ucsusa.org/resources/reviving-dead-zone>.
- J. G. P. W. Clevers. The derivation of a simplified reflectance model for the estimation of leaf area index. *Remote Sensing of Environment*, 25(1):53–69, June 1988. ISSN 0034-4257. doi: 10.1016/0034-4257(88)90041-7. URL <https://www.sciencedirect.com/science/article/pii/0034425788900417>.
- Jana E. Compton, John A. Harrison, Robin L. Dennis, Tara L. Greaver, Brian H. Hill, Stephen J. Jordan, Henry Walker, and Holly V. Campbell. Ecosystem services altered by human changes in the nitrogen cycle: a new perspective for US decision making. *Ecology Letters*, 14(8):804–815, 2011. ISSN 1461-0248. doi: 10.1111/j.1461-0248.2011.01631.x. URL <https://onlinelibrary.wiley.com/doi/abs/10.1111/j.1461-0248.2011.01631.x>. eprint: <https://onlinelibrary.wiley.com/doi/pdf/10.1111/j.1461-0248.2011.01631.x>.
- R. Escadafal. Remote sensing of arid soil surface color with Landsat thematic mapper. *Advances in Space Research*, 9(1):159–163, January 1989. ISSN 0273-1177. doi: 10.1016/0273-1177(89)90481-X. URL <https://www.sciencedirect.com/science/article/pii/027311778990481X>.
- North Carolina Cooperative Extension. PFP21: Think About Pests When Terminating Cover Crops Prior to Planting Soybeans, 2021. URL <https://soybeans.ces.ncsu.edu/2021/03/pfp21-think-about-pests-when-terminating-cover-crops-prior-to-planting-soybeans/>.
- Anatoly A. Gitelson, Yoram J. Kaufman, and Mark N. Merzlyak. Use of a green channel in remote sensing of global vegetation from EOS-MODIS. *Remote Sensing of Environment*, 58(3):289–298, December 1996. ISSN 0034-4257. doi: 10.1016/S0034-4257(96)00072-7. URL <https://www.sciencedirect.com/science/article/pii/S0034425796000727>.
- A Huete, K Didan, T Miura, E. P Rodriguez, X Gao, and L. G Ferreira. Overview of the radiometric

- and biophysical performance of the MODIS vegetation indices. *Remote Sensing of Environment*, 83(1):195–213, November 2002. ISSN 0034-4257. doi: 10.1016/S0034-4257(02)00096-2. URL <https://www.sciencedirect.com/science/article/pii/S0034425702000962>.
- A. R. Huete. A soil-adjusted vegetation index (SAVI). *Remote Sensing of Environment*, 25(3):295–309, August 1988. ISSN 0034-4257. doi: 10.1016/0034-4257(88)90106-X. URL <https://www.sciencedirect.com/science/article/pii/003442578890106X>.
- Carl F. Jordan. Derivation of Leaf-Area Index from Quality of Light on the Forest Floor. *Ecology*, 50(4):663–666, 1969. ISSN 1939-9170. doi: 10.2307/1936256. URL <https://onlinelibrary.wiley.com/doi/abs/10.2307/1936256>. eprint: <https://esajournals.onlinelibrary.wiley.com/doi/pdf/10.2307/1936256>.
- Meilin Ma, Carson Reeling, Megan N Hughes, Shalamar Armstrong, and Richard Roth. Comparison of conservation instruments under long-run yield uncertainty and farmer risk aversion. *European Review of Agricultural Economics*, 50(5):1685–1714, December 2023. ISSN 0165-1587. doi: 10.1093/erae/jbad029. URL <https://doi.org/10.1093/erae/jbad029>.
- Robert C. Marsett, Jiaguo Qi, Philip Heilman, Sharon H. Biedenbender, M. Carolyn Watson, Saud Amer, Mark Weltz, David Goodrich, and Roseann Marsett. Remote Sensing for Grassland Management in the Arid Southwest. *Rangeland Ecology & Management*, 59(5):530–540, September 2006. ISSN 1550-7424. doi: 10.2111/05-201R.1. URL <https://www.sciencedirect.com/science/article/pii/S1550742406500600>.
- Konstantinos Metaxoglou and Aaron Smith. Agriculture's nitrogen legacy. *Journal of Environmental Economics and Management*, 130:103132, March 2025. ISSN 0095-0696. doi: 10.1016/j.jeem.2025.103132. URL <https://www.sciencedirect.com/science/article/pii/S0095069625000166>.
- M. Duane Nellis and John M. Briggs. Transformed Vegetation Index for Measuring Spatial Variation in Drought Impacted Biomass on Konza Prairie, Kansas. *Transactions of the Kansas Academy of Science (1903-)*, 95(1/2):93–99, 1992. ISSN 00228443, 19385420. URL <http://www.jstor.org/stable/3628024>. Publisher: Kansas Academy of Science.
- Ariel Ortiz-Bobea. The Role of Nonfarm Influences in Ricardian Estimates of Climate Change Impacts on US Agriculture. *American Journal of Agricultural Economics*, 102(3):934–959, 2020. ISSN 1467-8276. doi: 10.1093/ajae/aaz047. URL <https://onlinelibrary.wiley.com/doi/abs/10.1093/ajae/aaz047>. eprint: <https://onlinelibrary.wiley.com/doi/pdf/10.1093/ajae/aaz047>.
- Marcel Pouget, J Madeira, E Le Floch, and S Kamal. Caracteristiques spectrales des surfaces sableuses de la region cotiere nord-ouest de l'Egypte: Application aux donnees satellitaires SPOT. *Caracterisation et suivi des milieux terrestres en regions arides et tropicales*, pages 27–39, 1991.
- J. Qi, A. Chehbouni, A. R. Huete, Y. H. Kerr, and S. Sorooshian. A modified soil adjusted vegetation index. *Remote Sensing of Environment*, 48(2):119–126, May 1994a. ISSN 0034-4257. doi: 10.1016/0034-4257(94)90134-1. URL <https://www.sciencedirect.com/science/article/pii/0034425794901341>.
- Jiaguo Qi, Y Kerr, and Abdelghani Chehbouni. External factor consideration in vegetation index development. *Proc. of Physical Measurements and Signatures in Remote Sensing, ISPRS*, 723:730, 1994b.
- BARRETT N ROCK. Field and airborne spectral characterization of suspected acid deposition

damage in red spruce (*Picea rubens*) from Vermont. In *Proc. Symp. on Machine Processing Remotely Sensed Data*, pages 71–81. Purdue Univ., 1985.

Gabrielle E. Roesch-McNally, Andrea D. Basche, J.G. Arbuckle, John C. Tyndall, Fernando E. Miguez, Troy Bowman, and Rebecca Clay. The trouble with cover crops: Farmers' experiences with overcoming barriers to adoption. *Renewable Agriculture and Food Systems*, 33(4):322–333, August 2018. ISSN 1742-1705, 1742-1713. doi: 10.1017/S1742170517000096. URL https://www.cambridge.org/core/product/identifier/S1742170517000096/type/journal_article.

JW Rouse, RdH Haas, and JA Schell. &Deering DW (1973). Monitoring vegetation systems in the Great Plains with ERTS. In *Third ERTS Symposium*, NASA, 1974.

W. P. M. Sawadgo, W. Zhang, and A. Plastina. What drives landowners' conservation decisions? Evidence from Iowa. *Journal of Soil and Water Conservation*, 76(3):211–221, May 2021. ISSN 0022-4561, 1941-3300. doi: 10.2489/jswc.2021.00115. URL <https://www.jswconline.org/content/76/3/211>. Publisher: Soil and Water Conservation Society Section: Research Section.

Wolfram Schlenker and Michael J. Roberts. Nonlinear temperature effects indicate severe damages to U.S. crop yields under climate change. *Proceedings of the National Academy of Sciences*, 106(37):15594–15598, September 2009. doi: 10.1073/pnas.0906865106. URL <https://www.pnas.org/doi/abs/10.1073/pnas.0906865106>. Publisher: Proceedings of the National Academy of Sciences.

Wolfram Schlenker, W. Michael Hanemann, and Anthony C. Fisher. The Impact of Global Warming on U.S. Agriculture: An Econometric Analysis of Optimal Growing Conditions. *The Review of Economics and Statistics*, 88(1):113–125, February 2006. ISSN 0034-6535. doi: 10.1162/rest.2006.88.1.113. URL <https://doi.org/10.1162/rest.2006.88.1.113>.

C. A. Taylor and Geoffrey Heal. Algal Blooms and the Social Cost of Fertilizer. 2021.

Compton J. Tucker. Red and photographic infrared linear combinations for monitoring vegetation. *Remote Sensing of Environment*, 8(2):127–150, May 1979. ISSN 0034-4257. doi: 10.1016/0034-4257(79)90013-0. URL <https://www.sciencedirect.com/science/article/pii/0034425779900130>.

Hans J. M. Van Grinsven, Mike Holland, Brian H. Jacobsen, Zbigniew Klimont, Mark a. Sutton, and W. Jaap Willem. Costs and Benefits of Nitrogen for Europe and Implications for Mitigation. *Environmental Science & Technology*, 47(8):3571–3579, April 2013. ISSN 0013-936X. doi: 10.1021/es303804g. URL <https://doi.org/10.1021/es303804g>. Publisher: American Chemical Society.

H. Von Blottnitz, A. Rabl, D. Boiadzhiev, T. Taylor, and S. Arnold. Damage costs of nitrogen fertilizer in Europe and their internalization. *Journal of Environmental Planning and Management*, 49(3):413–433, May 2006. ISSN 0964-0568. doi: 10.1080/09640560600601587. URL <https://doi.org/10.1080/09640560600601587>. Publisher: Routledge _eprint: <https://doi.org/10.1080/09640560600601587>.

Xiangming Xiao, Qingyuan Zhang, Bobby Braswell, Shawn Urbanski, Stephen Boles, Steven Wofsy, Berrien Moore, and Dennis Ojima. Modeling gross primary production of temperate deciduous broadleaf forest using satellite images and climate data. *Remote Sensing of Environment*, 91(2):256–270, May 2004. ISSN 0034-4257. doi: 10.1016/j.rse.2004.03.010. URL <https://www.sciencedirect.com/science/article/pii/S0034425704000975>.